

RAF Kinases: Pathway, Modulation and Modeling

Dissertation zur Erlangung des naturwissenschaftlichen
Doktorgrades der Bayerischen Julius-Maximilians-Universität
Würzburg

vorgelegt von

Armin Robubi

aus

Teheran, Iran

Würzburg 2007

Eingereicht am:

Mitglieder der Promotionskommission:

Vorsitzender: Prof. Dr. Martin J. Müller
Gutachter : Prof. Dr. Thomas Dandekar
Gutachter: Prof. Dr. Ulf R. Rapp

Tag des Promotionskolloquiums:

Doktorurkunde ausgehändigt am:

RAF Kinases: Pathway, Modulation and Modeling

Armin Robubi
Department of Bioinformatics
University of Würzburg

December 12, 2007

I dedicate this work to my mother.

Plain question and plain answer make the shortest road out of most perplexities.

Mark Twain

Abstract

The Ras/RAF/MEK/ERK cascade is a central cellular signal transduction pathway involved in cell proliferation, differentiation, and survival where RAF kinases are pivotal kinases implicated in cancer.

The development of specific irreversible kinase inhibitors is a rewarding but difficult aim. CI-1033 was developed to irreversibly inhibit erbB receptor tyrosine kinases by reacting to the Cys113 residue (p38 α MAP kinase numbering) of the kinase domain. In this study we tried a similar approach to target the RAF oncoproteins which possess a similar cysteine at position 108 in the hinge region between the small n-lobe and the large c-lobe of the kinase domain. A novel synthetic approach including a lyophilization step allowed us the synthesis of a diphenyl urea compound with an epoxide moiety (compound **1**). Compound **1** possessed inhibitory activity *in vitro*. However our time kinetics experiments and mass spectroscopic studies clearly indicate that compound **1** does not react covalently with the cysteine residue in the hinge region. Moreover, in cell culture experiments, a strong activation of the RAF signaling pathway was observed, an effect which is known from several other RAF kinase inhibitors and is here reported for the first time for a diphenyl urea compound, to which the clinically used unspecific kinase inhibitor BAY 43-9006 (Sorafenib[®], Nexavar[®]) belongs. Although activation was apparently independent on B- and C-RAF hetero-oligomerization *in vitro*, *in vivo* experiments support such a mechanism as the activation did not occur in starved knockout cells lacking either B-RAF or C-RAF (Robubi et al., ChemMedChem–submitted).

Furthermore, we developed a mathematical model of the Ras/RAF/MEK/ERK cascade demonstrating how stimuli induce different signal patterns and thereby different cellular responses, depending on cell type and the ratio between B-RAF and C-RAF. Based on biochemical data for activation and dephosphorylation, we set up differential equations for a dynamical model of the Ras/RAF/MEK/ERK cascade. We find a different signaling pattern and response result for B-RAF (strong activation, sustained signal) and C-RAF (steep activation, transient signal). We further support the significance of such

differential modulatory signaling by showing different RAF isoform expression in various cell lines and experimental testing of the predicted kinase activities in B-RAF, C-RAF as well as mutated versions (Robubi et al., 2005).

Additionally the effect of the tumor suppressor DiRas3 (also known as Noey2 or ARHI) on RAF signaling was studied. I could show that DiRas3 down-regulates the mitogenic pathway by inhibition of MEK (Beck, Robubi et al., Mol. Cell–submitted), a basis for a refined model of the Ras/RAF/MEK/ERK cascade (Robubi et al., in preparation).

Zusammenfassung

Die Ras/RAF/MEK/ERK Kaskade ist ein zentraler zellulärer Signalweg, der bei der Regulierung der Proliferation, Differenzierung und Überleben der Zelle eine entscheidende Rolle spielt. Dabei kommt den RAF Kinasen eine Schlüsselrolle bei der Tumorgenese zu.

Die Entwicklung von spezifischen irreversiblen Kinasehemmern stellt einen attraktiven, jedoch schwierigen Ansatz zur Tumorsuppression dar. CI-1033 wurde erfolgreich mit dem Ziel entwickelt, ErbB-Rezeptor-Tyrosinkinasen irreversibel zu inhibieren, indem es kovalent mit dem Cys113 (p38 α MAP Kinase Nummerierung) in der Kinase-Domäne reagiert. In dieser Arbeit wird ein vergleichbarer Ansatz gegen die RAF-Onkoproteine verfolgt, die einen analogen Cystein-Rest in der Position 108 aufweisen. Dieser ist in der Hinge-Region zwischen dem kleinen n-lobe und dem großen c-lobe der Kinase-Domäne lokalisiert. Ein neuer synthetischer Ansatz, der einen Lyophilisierungsschritt mit einschloss, erlaubte hierfür die Synthese einer Diphenylharnstoff-Verbindung mit einer Epoxidgruppe (Verbindung **1**).

Verbindung **1** zeigt *in vitro* tatsächlich eine inhibitorische Aktivität gegen RAF-Kinasen. Jedoch zeigen unsere zeitkinetischen Experimente, sowie unsere massenspektrometrischen Analysen, dass Verbindung **1** keine kovalente Bindung mit dem Cystein-Rest in der Hinge-Region bildet. Außerdem stellten wir in Zellkulturexperimenten eine starke Aktivierung des RAF-induzierten Signalweges fest; ein Effekt, der bereits für andere RAF-Kinase-Inhibitoren beschrieben wurde, jedoch hier erstmalig auch für eine Diphenylharnstoff-Verbindung, zu der auch BAY 43-9006 (Sarafinib[®], Nexavar[®]) gehört. BAY 43-9006 ist ein unspezifischer, für die Behandlung von Krebs zugelassener, Kinase Inhibitor. Obwohl die Aktivierung *in vitro* scheinbar unabhängig von einer Heterooligomerisierung von B-RAF und C-RAF war, unterstützen *in vivo* Experimente einen solchen Mechanismus, da in gehungerten knockout Zellen, in denen B-RAF oder C-RAF fehlte, keine Aktivierung beobachtet werden konnte (Robubi et al., ChemMedChem–eingereicht).

Des Weiteren zeigten wir in einem mathematischen Modell, wie abhängig vom B-RAF/C-RAF-Verhältnis verschiedene Zellantworten durch unterschied-

liche Stimuli induzierbar werden. Basierend auf biochemischen Daten über Aktivierung und Dephosphorylierung sowie auf den Differentialgleichungen unseres Rechenmodells fanden wir eine unterschiedliche Signalkinetik für B-RAF (starke Aktivierung, anhaltendes Signal) und C-RAF (schwache Aktivierung, transientes Signal). Die Bedeutung dieser differenzierten Signalmodifikation wurde auch durch unterschiedliche Expression der RAF Isoformen in verschiedenen Zelllinien und durch die experimentelle Messung der Kinaseaktivität von B- und C-RAF sowie mutierte Formen überprüft (Robubi et al., 2005).

Zusätzlich wurde der Effekt des Tumorsuppressorproteins DiRas3 (auch bekannt als Noey2 oder ARHI) auf den RAF-Signalweg untersucht. Wir konnten zeigen, dass DiRas3 den mitogenen Signalweges durch Inhibierung der mitogen-aktivierten Proteinkinase Kinase (MEK) negativ reguliert (Beck, Robubi, et al., Mol. Cell–eingereicht), eine Basis für ein verfeinertes Modell der Ras/RAF/MEK/ERK Kaskade (Robubi et al., in Vorbereitung).

Contents

Abstract	V
Zusammenfassung	VII
1 Introduction	19
1.1 History and nomenclature of RAF kinases	19
1.2 RAF kinase signaling	22
1.3 Mouse knockout models	23
1.4 RAF kinases in cancer	23
1.5 Architecture of Raf kinases	25
1.5.1 Kinase domain	25
1.6 Development of a novel RAF kinase inhibitor	28
1.7 Dynamic pathway modeling	29
1.8 DiRas3	30
2 Materials and Methods	33
2.1 Compound characterization	33
2.2 Cell culture	33
2.2.1 Conditions for inhibitor studies	33
2.2.2 Conditions used for modeling studies	33
2.3 Immuno blot analysis	34
2.4 Kinase assay (immuno blot)	34
2.5 Kinase assay (ELISA)	35
2.6 Kinase assay (DiRas3)	36
2.7 Biosensor measurements	36
2.8 Mass spectrometry measurements	36
2.9 Gel filtration	37
2.10 Bioinformatics	37
2.10.1 Molecular modeling	37
2.10.2 Dynamic pathway modeling	38

3	Results	39
3.1	Development of a novel RAF kinase inhibitor	39
3.1.1	Homology modeling	39
3.1.2	Activity of compound 1 <i>in vitro</i>	43
3.1.3	Activation in cell culture	44
3.1.4	Other compounds	47
3.2	Dynamic modeling	49
3.3	DiRas3	58
3.3.1	DiRas3 interacts <i>in vitro</i> efficiently with active C-RAF and MEK.	58
3.3.2	Inhibition of MEK activity by DiRas3 <i>in vitro</i>	59
4	Discussion	63
4.1	Developing a novel RAF kinase inhibitor	63
4.2	Dynamic modeling	66
4.3	DiRas3	68
	Bibliography	71
	Acknowledgments	85
	Curriculum vitae	87
	List of publications	89
	Poster Abstracts	90
	Oral presentations	91
A	Supplementary material	93
	Erklärung	95

List of Figures

1.1	Some important steps in RAF research.	20
1.2	Scheme of the mitogenic signaling pathway.	24
1.3	Multiple alignment of A-, B-, and C-RAF.	26
1.4	3D crystal structure of the kinase domain B-RAF.	27
1.5	RAF kinase inhibitors	28
3.1	Development of a new lead compound.	40
3.2	Model of compound 1 in complex with B-RAF.	41
3.3	Synthesis of compound 1	42
3.4	Inhibition of RAF kinases in an <i>in vitro</i> kinase assay.	44
3.5	Time kinetics experiment.	45
3.6	Mass spectrometry data	46
3.7	Elevated levels of pERK after treatment with compound 1	47
3.8	No activation by compound 1 in starved RAF knockout cells.	48
3.9	Hetero-oligomerization of B-RAF and C-RAF <i>in vitro</i>	48
3.10	Synthesis of compounds 10 and 16	50
3.11	Model of the Ras-ERK signaling pathway; depiction of the parameters.	52
3.12	Response curve for the Ras-ERK pathway under standard conditions.	53
3.13	Simulation showing the qualitative differences between B-RAF and C-RAF.	54
3.14	Gel showing different expression levels of RAF kinases in different tissues.	55
3.15	Kinase assays showing the activity of different preparations of RAF kinases.	56
3.16	DiRas3 interaction with C-RAF and MEK—BIAcore.	59
3.17	DiRas3 interaction with C-RAF and MEK—summary.	60
4.1	Reaction mechanism between a cysteine and an epoxide.	63
4.2	Model of the mitogenic signaling pathway.	65

4.3	DiRas3 binds to RAF as well as to MEK and blocks MEK from phosphorylating ERK.	69
A.1	Scanning different parameter values.	94

List of Tables

1.1	Nomenclature of RAF kinases	21
1.2	Cellular signals and responses.	30
3.1	Inhibition of C-RAF and MEK by different inhibitors <i>in vitro</i>	51
3.2	Parameter values.	55

List of Abbreviations

SI-Units are not listed.

®	registered
3D	three dimensional
A	adenine/adenosine
AA	amio acid
abs.	absolute
AML	acute myeloid leukemia
ANP	atrial natriuretic peptide receptor
ATP	adenosine 5'-triphosphate
ATR	attenuated total reflectance
BLK	block residue as defined in the MODELLER package
Boc ₂ O	di-tert-butyl dicarbonate
bp	base pair
BSA	bovine serum albumin
C	cytosine, cysteine
c-lobe	C-terminal lobe
CFC	cardio-facio-cutaneous
CR1, 2, 3	conserved region 1, 2, 3
CRD	cysteine rich domain
Cys	cysteine
D	aspartate
Da	dalton
DFG	aspartate-phenylalanine-glycine
DMAP	4-dimethylaminopyridine
DMEM	dulbecco's modified eagle medium
DMSO	dimethyl sulfoxide
DNA	deoxyribonucleic acid
DTT	dithiothreitol
E	glutamate

ECL	enhanced chemoluminescence
<i>E. coli</i>	<i>Escherichia coli</i>
EDTA	ethylenediamine tetraacetic acid
e.g.	for example; Lat.: <i>exempli gratia</i>
EGF	epidermal growth factor
EGFR	epidermal growth factor receptor
ELISA	enzyme-linked immunosorbent assay
ERK	extracellular signal-regulated kinase
Et ₂ O	diethyl ether
Et ₃ N	triethyl amine
EtOH	ethanol
FCS	fetal calf serum
FDA	food and drug administration
FGF	fibroblast growth factor
FRS2	fibroblast growth factor receptor substrate 2
FT-IR	fourier transform infrared
G-loop	glycine rich loop
GAP	GTPase activating protein, GTPase accelerating protein
GDP	guanosine diphosphate
GEF	guanine nucleotide exchange factor
Grb2	growth factor receptor-bound protein 2
GS	glutathione sepharose
GST	glutathione S-transferase
GTP	guanosine triphosphate
HEK293	human embryonic kidney cells
Hepes	4-(2-hydroxyethyl)-1-piperazineethanesulfonic acid
HS	horse serum
JNK	c-Jun N-terminal kinase
KSR	kinase suppressor of Ras
Lck	eukocyte-specific protein tyrosine kinase
MA	Massachusetts
MAPK	mitogen-activated protein kinase
MAPKK	mitogen-activated protein kinase kinase
MAPKKK	mitogen-activated protein kinase kinase kinase
MDR	multi drug resistance
MEK	mitogen-activated protein kinase kinase
MeOH	methanol
Mg-loop	magnesium positioning loop
MH2	Mil-Hill No. 2
MSV	mouse sarcoma virus
MTP	micro titer plate

n-lobe	N-terminal lobe
NGF	nerve growth factor
Ni-NTA	nickel-nitrilotriacetic acid
NP40	nonidet 40
NR	n-region
NSCLC	non-small-cell lung cancer
ODE	ordinary differential equation
OMIM	online mendelian inheritance in man
OPD	o-phenylenediamine hydrochloride
PAGE	sodium dodecyl sulfate polyacrylamide gel electrophoresis
PBS	phosphate buffered saline
PC12	rat pheochromocytoma
PDB	protein data bank
PDGFR	platelet-derived growth factor receptor
PMA	phorbol 12-myristate 13-acetate
PNS	post-nuclear supernatant
RAF	rapidly growing fibrosarcoma
RAF-ER	RAF-estrogen receptor
RBD	Ras binding domain
RET	rearranged during transfection
RNA	ribonucleic acid
RPMI	roswell park memorial institute medium 1640
r.t.	room temperature
RTK	receptor tyrosine kinase
RU	response units
SDS	sodium dodecyl sulfate
Ser	serine
SHC	Src homology 2 domain (or SH2 domain)
si-oligos	small interfering oligonucleotides
siRNA	small interfering RNA
SOS	son of sevenless
Speg	striated muscle-specific serine/threonine protein kinase
T	threonine
TBST	tris-buffered saline Tween-20
TCA	trichloroacetic acid
TFA	trifluoroacetic acid
THF	tetrahydrofuran
Thr	threonine
TPA	tetradecanoylphorbol acetate
Tyr	tyrosine
VEGFR	vascular endothelial growth factor receptor

wt	wild type
Y	tyrosine

Chapter 1

Introduction

RAF kinases are an important group of proto-oncoproteins. They play a key role in the mitogenic signaling pathway (Ras/RAF/MEK/ERK), a highly conserved signaling pathway which controls proliferation, differentiation and survival. The mitogenic signaling pathway was found to be hyper-regulated in about 30% of solid tumors (Hoshino et al., 1999). Ras, a small GTP binding protein, is a common proto-oncoprotein that binds directly to RAF kinases and initiates a highly complex process of activation. RAF kinases are the best studied effectors of Ras. The fact that B-RAF mutations were also found in human cancers underlines their prominent role in oncogenesis (Davies et al., 2002).

My project covers a wide range of issues around RAF kinases. (i) It started from structural analysis of the kinase domain of B-RAF followed by an effort to develop a novel irreversible RAF kinase inhibitor. Three novel compounds were synthesized and their behavior against RAF kinases were studied. (ii) A mathematical model was developed to study dynamic properties of the Ras/RAF/MEK/ERK signaling pathway. (iii) Additionally the interaction of RAF kinases with the tumor suppressor DiRas3 (also known as Noey2/ARHI) was studied. I could show that DiRas3 downregulates the mitogenic pathway by inhibition of the mitogen-activated protein kinase kinase (MEK), which is the major substrate of RAF kinases. This provides a basis for a refined model of the cascade signaling.

1.1 History and nomenclature of RAF kinases

Figure 1.1 winds up important milestones in the research of RAF kinases.

The oncogene of the acutely transforming replication-defective mouse type C virus 3611-MSV was characterized in 1983 (Rapp et al., 1983). Since 3611-

MSV induces rapidly growing fibrosarcomas, the transforming viral oncogene was called *v-raf*. Its cellular homologs in mouse and in human were therefore called *c-raf-1* and *c-raf-2*, respectively.

In the same year the avian acute leukemia retrovirus Mil-Hill No. 2 (MH2) was found to carry a second oncogene in addition to *v-myc*, which was termed *v-mil* after the virus. Its cellular homolog was termed *c-mil* (Jansen et al., 1983). *c-mil* turned out to be the avian homolog of the mammalian *c-raf* (Jansen et al., 1984). *c-raf-2* later turned out to be a pseudogene (Bonner et al., 1985). The product of the *c-raf-1* gene became c-Raf-1 (e.g. c-raf-1, craf1, C-Raf-1) or just Raf-1.

In 1986 a new paralog of *c-Raf-1* was found and termed *A-Raf* according to the nomenclature of that time. Two *A-Raf* genes were found in humans and mice and termed *A-Raf-1* and *A-Raf-2* (Huebner et al., 1986). *A-Raf-1* is a functional gene located on chromosome X, whereas *A-Raf-2* is a pseudogene.

Finally, in 1988, a second paralog of *c-Raf* was identified as a homolog of transforming gene in a human Ewing sarcoma (Ikawa et al., 1988). Also in 1988, the avian homolog of *c-mil* was identified and found to transform neuroretinal cells in chicken. It was termed *c-Rmil* to point out its retinal origin and its homology with *c-mil* (the chicken has no ortholog of *A-Raf*). As with the other Raf isoforms two *B-Raf* genes were found in human. One (B1) being functional, the other (B2) being a pseudogene (Sithanandam et al., 1992).

Table 1.1 summarizes the different nomenclatures of RAF kinases. Recently Wellbrock et al. (2004) suggested a nomenclature using A-RAF, B-RAF and C-RAF for the functional proteins and *A-RAF*, *B-RAF*, *C-RAF* for the corresponding genes in human and A-Raf, B-Raf and C-Raf (and *A-Raf*,

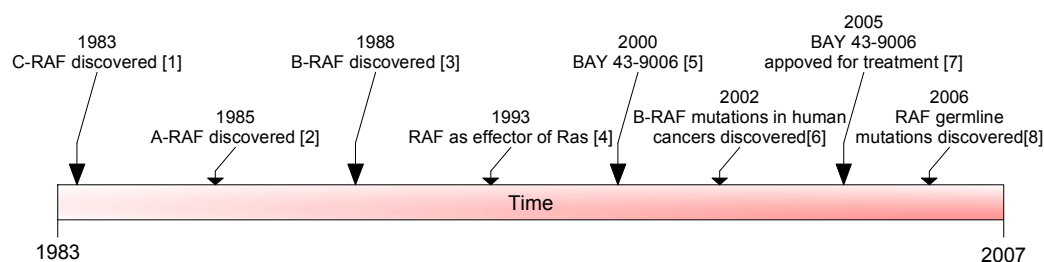


Figure 1.1: **Some important steps in RAF research.** The time bar shows, starting from the discovery of C-RAF, the major discoveries in RAF research with references: 1: Rapp et al. (1983), 2: Huebner et al. (1986), Ikawa et al. (1988), 4: Zhang et al. (1993), 5: Lowinger et al. (2002), 6: Davies et al. (2002), 7: Strumberg et al. (2007), 8: Duesbery and Woude (2006).

In this work	Alternative names	Hugo names
A-RAF	A-Raf, A-Raf-1, araf	<i>araf</i>
B-RAF	B-Raf, braf, BRAF, BRAF1, B-Raf-1, c-Rmil, p94, v-Raf murine sarcoma viral oncogene homolog B1	<i>braf</i>
C-RAF	Raf-1, craf, craf1, cRaf-1, c-Raf-1, c-mil, v-raf-1 murine leukemia viral oncogene homolog 1, v-raf murine sarcoma 3611 viral oncogene homolog	<i>craf1</i>

Table 1.1: Nomenclature of RAF kinases

B-Raf, *C-Raf*) for the corresponding murine proteins (and genes). Hereafter I will use the former spelling throughout the entire thesis.

RAF kinases were found to bind directly to the small GTP binding protein Ras (Koide et al., 1993; Zhang et al., 1993). Ras proteins were well established proto-oncoproteins and Ras mutations were already found in many human cancers (Malumbres and Barbacid, 2003). Thus RAF kinases—particularly C-RAF—were intensively studied in the following years.

BAY 43-9006 (Sorafenib[®], Nexavar[®]) is a C-RAF targeted small molecule kinase inhibitor developed by the pharmaceutical company Bayer[®] (Lowinger et al., 2002). It entered clinical trials in 2002 (Richly et al., 2003; Gollob et al., 2005; Strumberg et al., 2007). The drug received FDA approval in December 2005 for the treatment of patients with advanced renal cell carcinoma and more recently—in November 2007—for the treatment of advanced hepatocellular carcinoma. BAY 43-9006 is not a specific C-RAF inhibitor but shows activity against a wide range of protein kinases including other RAF kinase isoforms, as well as a number of tyrosine kinases such as platelet-derived growth factor receptor β (PDGFR- β), vascular endothelial growth factor receptors (VEGFR-1 and VEGFR-2), Flt-3, and c-Kit (Wilhelm et al., 2004) as well as rearranged during transfection (RET) (Carlomagno et al., 2006).

Davies et al. (2002) demonstrated that mutations of the *B-RAF* gene occur in a high number of human tumors, moving the attention somewhat from C-RAF.

Mouse models demonstrated that the mitogenic signaling pathway was of crucial importance for cellular function and for development. Germ line mutations with strong impact in one or the other way were considered to be lethal during embryonal development. It was thus a real surprise for the scientific community when gain-of-function mutations in key components of that pathway were reported to cause mendelian disorders in human (Duesbery

and Woude, 2006). Cardio-facio-cutaneous (CFC) syndrome (OMIM#115150) is caused by activating mutations of either the *K-Ras*, *B-RAF*, *MEK-1*, or *MEK-2* gene. Interestingly the gain-of-function mutations in *B-RAF* are distinct from the ones observed in cancer (Rodriguez-Viciano et al., 2006). The CFC syndrome overlaps clinically with Costello syndrome (OMIM#218040) which is caused by gain-of-function mutations of the *H-Ras* gene (Aoki et al., 2005). Germ line mutations of the *C-RAF* gene have also been reported in causing acute myeloid leukemia (AML) (Zebisch et al., 2006).

1.2 RAF kinase signaling

The mitogenic signaling pathway is shown in Figure 1.2. Receptor tyrosine kinases (RTKs) bind growth factors in the extracellular space. This binding leads to their oligomerization and trans-phosphorylation. The growth factor receptor-bound protein 2 (Grb2) binds to the phosphorylated RTKs through its SHC domain. The signal is passed over to the G-protein exchange factor (GEF) son of sevenless (SOS). SOS facilitates the nucleotide exchange of Ras, replacing its GDP by GTP. Ras-GTP recruited RAF kinases as well as a number of other effectors. RAF kinases bind to Ras-GTP (Koide et al., 1993; Zhang et al., 1993) after which a complex ensemble of kinases, phosphatases, scaffold proteins, and lipids is required for their activation. For all RAF isoforms, the exact mechanism of activation has not been fully elucidated. The activation of C-RAF has been studied most intensively but is probably also the least understood.

Expression of constitutively active RAF kinase activates the extracellular signal-regulated kinase—ERK (Dent et al., 1992; Howe et al., 1992). ERK is not directly phosphorylated by RAF kinases but through the mitogen-activated protein kinase kinase (MEK). MEK is a dual specificity protein kinase which activates ERK by phosphorylating a tyrosine and a threonine residue in its activation segment. Thus RAF kinases act as MAP kinase kinase kinases (MAPKKKs) activating MEK, which in turn activates the MAP kinase ERK (Kyriakis et al., 1992).

Two isoforms of ERK are found in mammals: ERK-1 and ERK-2. The former has a molecular mass of 44 kDa, the latter 42 kDa. They share about 43% sequence identity and are expressed in varying extends in all tissues. Deletion of *ERK-2* leads to early embryonic lethality (Saba-El-Leil et al., 2003), whereas deletion *ERK-1* does not (Pagès et al., 1999), indicating that they have distinct functions. Two residues of the conserved TEY motive in the activation segment—T183 and Y185—need to be phosphorylated to fully activate ERK (Payne et al., 1991; Robbins et al., 1993). Mutation of

those amino acids to acidic residues is however not sufficient to generate a constitutively active kinase (Canagarajah et al., 1997).

MEK-1 and MEK-2 are the only protein kinases known so far to phosphorylate ERK-1 and ERK-2. In fact, ERK-1/2 are also the only MEK-1/2 substrates known so far. MEK is a dual specificity kinase which phosphorylates both required residues in the activation segment of ERK. MEK on the other hand, needs to be phosphorylated on two serine residues (S218, S222) of its activation segment—LIDSMANS—by RAF kinases to be active. Mutation of the two residues to acidic amino acids gives rise to a constitutively active kinase (S218E, S222E; LIDEMANE). *MEK-1* knock out mice die at an early embryonic stage (Giroux et al., 1999), whereas deletion of *MEK-2* gives no significant phenotype (Bélanger et al., 2003).

1.3 Mouse knockout models

The distinct functions of RAF kinase isoforms can be studied using mouse knockout models. Knockout mice for all three RAF isoforms have been generated. Surprisingly all three RAF isoforms appear to be very important. All RAF knockout mice display distinct but severe phenotypes with A-RAF knockouts showing the mildest phenotype (Pritchard et al., 1996; Mikula et al., 2001; Wojnowski et al., 1997).

This is rather surprising since other proteins in the signaling module exhibit redundancy to a much higher extent. Even in the case of Ras, only the *K-Ras* gene seems to be essential (Malumbres and Barbacid, 2003).

1.4 RAF kinases in cancer

In one study the mitogenic signaling pathway was shown to be upregulated in 50 of 138 human tumor cell lines (Hoshino et al., 1999). Upregulation can be caused by gain-of-function mutations or by overexpression of a number of proteins. Particularly Ras mutations are commonly found in tumors. However, a considerable number of tumors were shown to carry mutations in the *B-RAF* gene (Davies et al., 2002), in particular malignant melanoma (27–70%), papillary thyroid cancer (36–53%), colorectal cancer (5–22%), and serous ovarian cancer (~30%). Virtually all B-RAF mutations found in human cancers are located either in the N-terminal region of the activation segment or in the glycine rich loop (Figure 1.3). More than 40 different mutations of the B-RAF gene have been observed in human cancers. However a single thymine to adenine transversion accounts for about 90% of the cases. This

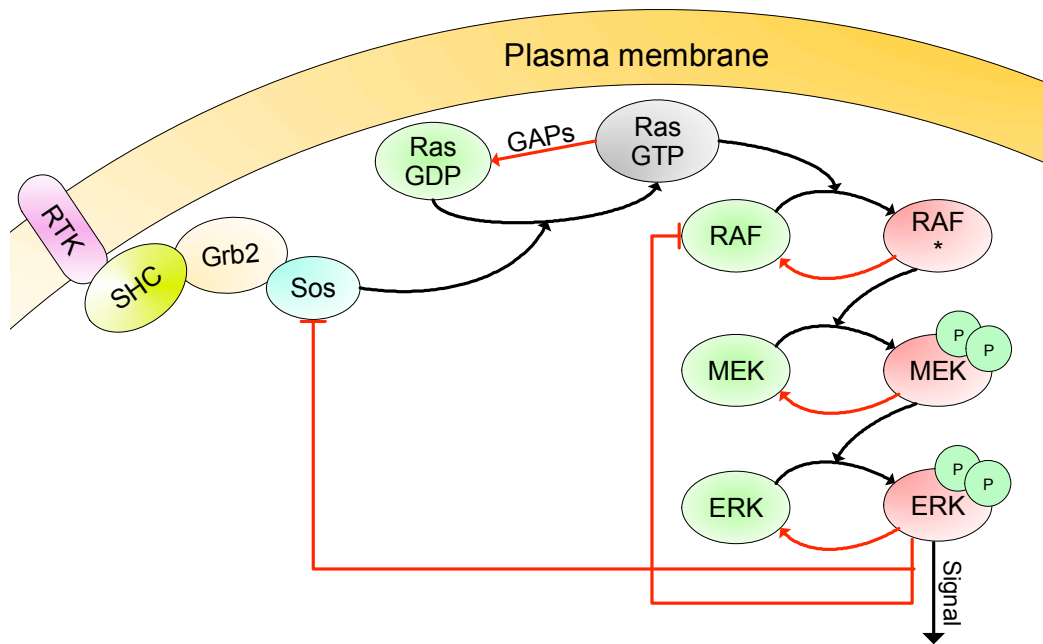


Figure 1.2: **Scheme of the mitogenic signaling pathway.** Growth factors bind to receptor tyrosine kinases (RTKs) inducing oligomerization and trans-phosphorylation. Growth factor receptor-bound protein 2 (Grb2) binds to the phosphorylated RTKs through its SHC domain. Son of sevenless (SOS) is activated by Grb2 and facilitates the nucleotide substitution of GDP by GTP bound by Ras proteins. Ras-GTP binds directly to RAF kinases, inducing a complex process of activation. Active RAF kinases activate the mitogen activated protein kinase kinase (MEK) by phosphorylation of two residues in the activation segment. Activated MEK in turn phosphorylates the extracellular signal-regulated kinase (ERK). Phosphorylated ERK has a large number of substrates and is involved in many cellular processes (Campbell et al., 1998). Negative feedback regulation by active ERK is described at the level of SOS and RAF kinases (Chen et al., 1996; Brummer et al., 2003; Dougherty et al., 2005; Hekman et al., 2005).

mutation converts a valine residue in the N-terminal region of the activation segment into a glutamate (B-RAF-V600E) and gives rise to a constitutively active kinase (Garnett and Marais, 2004).

1.5 Architecture of Raf kinases

RAF kinases are multi domain proteins. Most vertebrates possess three RAF isoforms referred to A-RAF, B-RAF, and C-RAF. The overall architecture of A-RAF, B-RAF, and C-RAF resemble each other. All three possess three highly conserved regions. CR1 at the N-terminus, CR3 at the C-terminus, and CR2 in between. CR3 encodes the kinase domain, the most conserved region (Figure 1.3).

RAF kinases are subject to complex regulation which is also reflected by the high number of phosphorylation sites which are distributed throughout the whole protein. While some phosphorylation sites are conserved throughout the whole protein family, others are not, indicating that different isoforms may be subject to distinct modes of regulation.

CR3 constitutes the catalytic kinase domain of the protein (Figure 1.4). Its sequence is highly conserved between different RAF isoforms and shows a higher sequence homology to tyrosine kinases than other serine/threonine kinases. Nevertheless RAF kinases appear to act as serine/threonine kinases exclusively.

CR2 contains the S256 (C-RAF numbering) residue which binds 14-3-3 proteins upon phosphorylation and is a major negative regulatory site (Hekman et al., 2004).

CR1 contains the Ras binding domain (RBD) and the cysteine rich domain (CRD) and is important for Ras-GTP and membrane association.

1.5.1 Kinase domain

The kinase domain is highly conserved between RAF paralogs and orthologs. The catalytic function of RAF kinases, that is the transfer of an orthophosphate from ATP to a protein, is solely depended on that domain. It is also the target of all current RAF kinase inhibitors, including the one developed in this work.

Tyrosine and serine/threonine kinases are structurally closely related. There are the largest family of proteins encoded by the human genome. Due to their high importance a large number of crystal structures of kinase domains were solved. Parts of the kinase domain of B-RAF could be solved with a resolution of 2.95 Å (Wan et al., 2004). The kinase domain has a structure

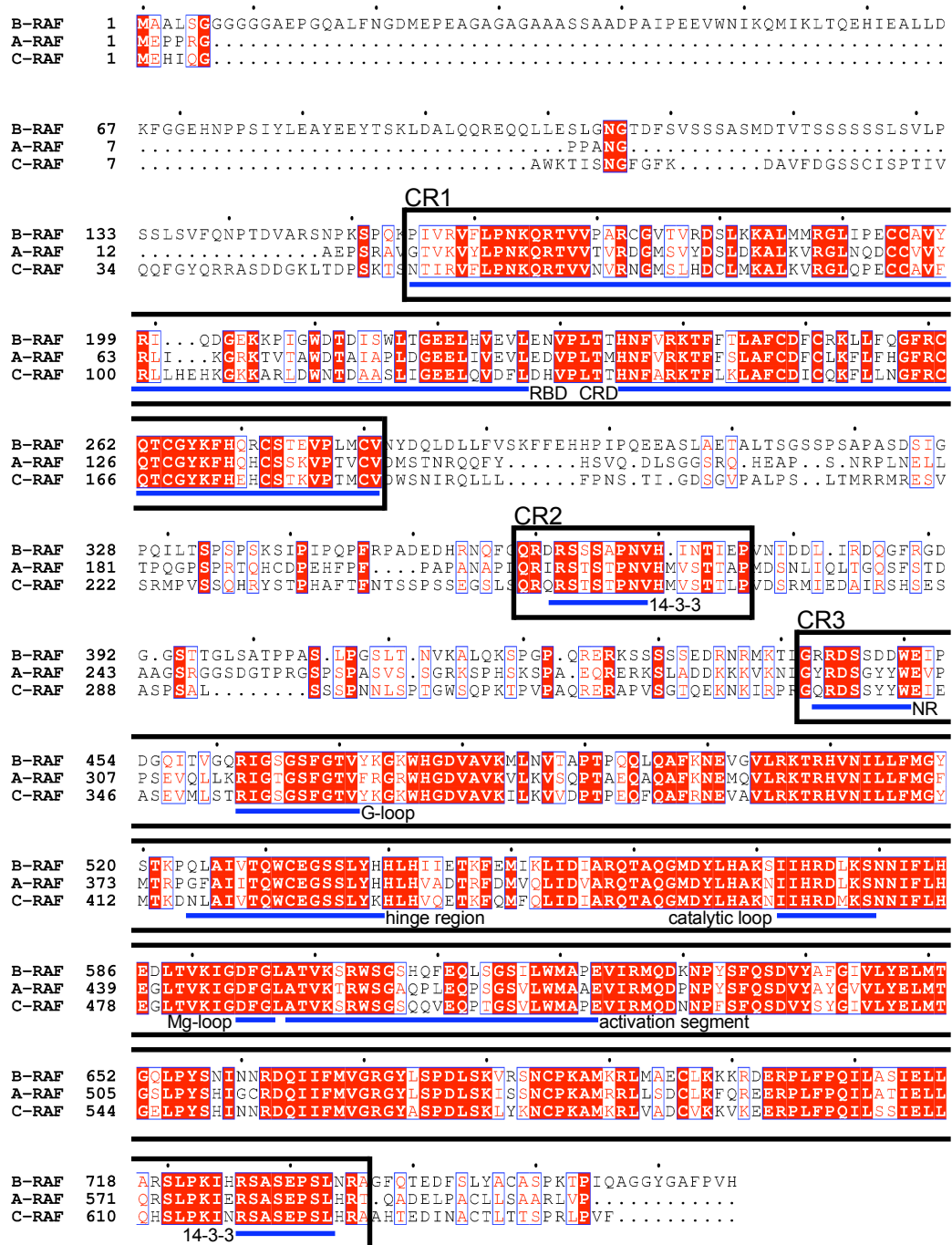


Figure 1.3: **Multiple alignment of A-, B-, and C-RAF.** Residue numbering (human sequences) is indicated on the left. Dots indicate every tenth B-RAF residue. Strictly conserved residues are shown as red blocks with white lettering. Similar positions are highlighted in red and boxed. Dots in the sequences indicate gaps. Indicated are the following motifs: CR1, CR2, and CR3. The N-terminal CR1 contains the Ras binding domain (RBD) and the cysteine rich domain (CRD). CR2 is situated in the middle of the protein and bears a conserved 14-3-3 binding site. CR3 contains the kinase domain with several important motives: the N-region (NR), the glycine rich loop (G-loop), the hinge region, the catalytic loop, the magnesium positioning loop (Mg-loop), the activation segment, and the C-terminal 14-3-3 binding site.

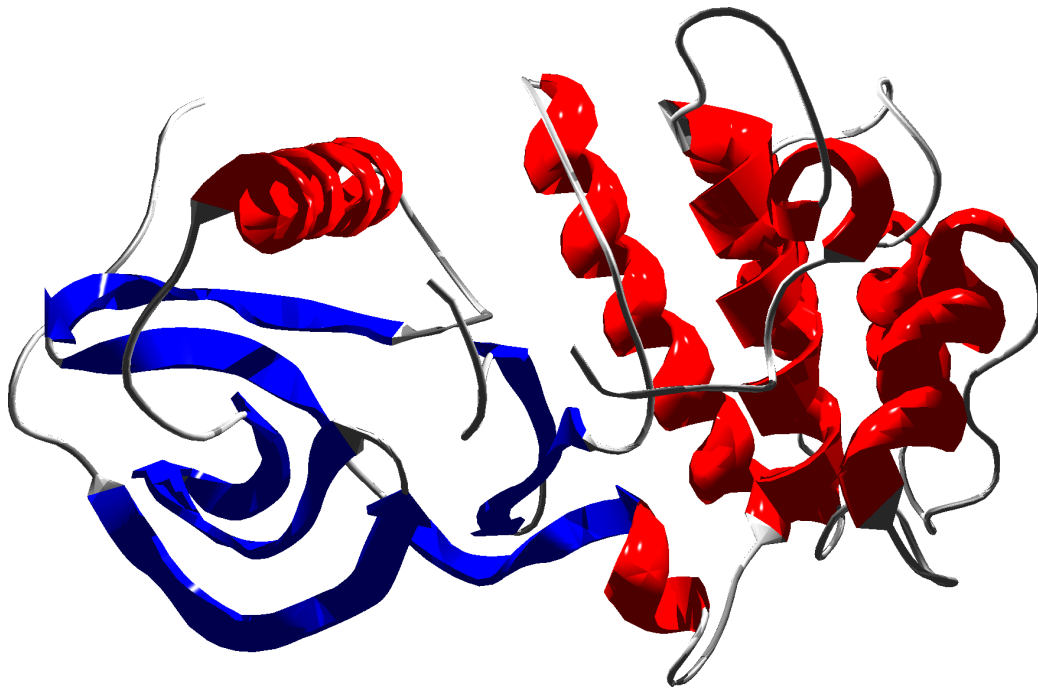


Figure 1.4: **3D crystal structure of the kinase domain B-RAF**. Image is based on the PDB entry 1UWH (Wan et al., 2004). All β -strands are shown in blue, α -helices in red. The kinase domain of RAF kinases resembles the general architecture of all serine/threonine/tyrosine kinases. It consists of a small N-terminal section (n-lobe; left) which is built up by three β -strands, an α -helix, and two further β -strands; and a large C-terminal lobe (c-lobe; right) which is predominantly built up by α -helices. The ATP molecule can be bound by the narrow cleft between the lobes. The stretch of the activation segment is quite flexible and is therefore not detectable in the electron density map of many crystal structures; this is also the case for the B-RAF crystal structure.

known from other serine/threonine/tyrosine protein kinases, as shown in the crystal structure in Figure 1.4. It consists of a small n-lobe which in turn is built up by five β -sheets and one α -helix and a larger c-lobe which is predominantly built up by α -helices. The ATP molecule is bound by the narrow cleft between the lobes. See also Figure 1.3 for the crucial residues in the kinase domain (CR3).

1.6 Development of a novel RAF kinase inhibitor

A number of compounds, which were developed as RAF kinase inhibitors do inhibit RAF kinases *in vitro* yet, paradoxically, activate RAF kinases in cell culture, independent of substance classes (Figure 1.5). These compounds include ZM 336372 (Hall-Jackson et al., 1999a), GW 5074 (Lackey et al., 2000; Chin et al., 2004) and SB 203580 (Hall-Jackson et al., 1999b). So far, only BAY 43-9006 (Sorafenib[®], Nexavar[®]), a diphenyl urea compound, passed clinical trials for cancer treatment. BAY 43-9006 acts, like most kinase inhibitors, in a reversible manner.

As here a bundle of different methods had to be combined, the complete strategy is briefly summarized here: (i) generate models of the kinase domain of B-RAF in complex with diphenyl urea ligands; (ii) synthesis of a novel diphenyl urea lead compound with an epoxide moiety; (iii) in depth biochemical characterization of the lead *in vitro* as well as in cell culture. We first generated a homology model of the kinase domain of B-RAF in complex with BAY 43-9006. Therein we observed a close proximity between the pyridine moiety of the inhibitor and a cysteine residue in the hinge region (Figure 1.3) of the kinase domain. Since few protein kinases possess a cysteine at this

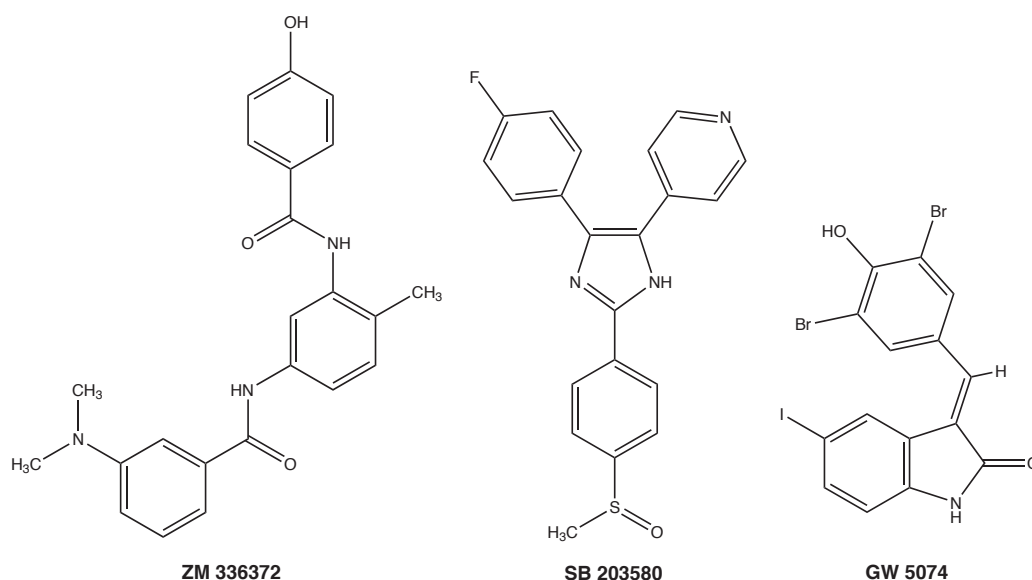


Figure 1.5: **RAF kinase inhibitors:** ZM 336372 (Hall-Jackson et al., 1999a), SB 203580 (Hall-Jackson et al., 1999b) and GW 5074 (Lackey et al., 2000; Chin et al., 2004).

position, we argued that it may be an attractive nucleophile to covalently link inhibitor molecules with mildly electrophilic groups to the kinase domain and thus irreversibly and specifically diminish the molecule's kinase activity. This led to the successful synthesis of a diphenyl urea lead compound with an epoxide moiety. We did not detect covalent binding to the targeted cysteine residue, which may be explained by sterical problems, although we did achieve inhibition of RAF kinase (B, C) at an IC_{50} of 1 and 100 μ M which is about three orders of magnitude higher than for BAY 43-9006. In contrast to BAY 43-9006, compound **1** strongly elevated the content of phosphorylated ERK in RAF transformed NIH 3T3 cells. This is the first report of a diphenyl urea compound activating RAF kinase *in vivo*. The underlying mechanism has not been definitively delineated. Although there was no evidence for the exact mechanism *in vitro*, *in vivo* data provide suggestive evidence for heterooligomer formation because no activation could be observed in starved knockout cells lacking B-RAF or C-RAF.

1.7 Dynamic pathway modeling

The high complexity of RAF kinase regulation offers more options for regulation than any other step of the pathway. The intensity and duration of kinase signals are important determinants (Table 1.2) for cellular responses (Marshall, 1995; Kerkhoff and Rapp, 1998). In PC12 rat pheochromocytoma cells, nerve growth factor (NGF) induces sustained activation of Ras (Qui and Green, 1992). The activity of the B-RAF isoform essentially follows Ras-GTP, whereas the C-RAF isoform, after strong initial activation, is quickly inactivated (Wixler et al., 1996). The prolonged activation of B-RAF causes sustained activation of the mitogenic signaling pathway, which inhibits cell growth and induces differentiation. On the other hand, epidermal growth factor (EGF) induces short activation of Ras (B-RAF and C-RAF). The resulting transient ERK activation stimulates cell growth (Tombes et al., 1998). In rat hepatocytes, both NGF and EGF induce phasic activation of C-RAF and sustained activation of B-RAF. However, with both growth factors, phasic activation of the mitogenic signaling pathway is observed, leading to increased cell growth. Sustained activation of ERK using a RAF-ER construct blocks cell growth, as in PC12 cells (Tombes et al., 1998).

We start from a mathematical formalism suggested by Heinrich et al. (2002). Conceptually, our model includes the following advances: (i) We consider the central RAF-MEK-ERK signaling pathway. To obtain accurate parameter estimations, the model presented here was carefully constructed, exploiting available experimental data on the RAF-kinase cascade (e.g. Ras-

GTP half-life). (ii) This new model considers the effect of kinase isoforms on signaling cascades, specifically B-RAF and C-RAF. (iii) Furthermore, we studied their differential inactivation by phosphatases. (iv) Including all these features, we can then theoretically model and experimentally show that differential expression and ratios of different RAF isoforms can partially explain different mitogenic signaling behavior in different cell types. This includes direct tests on the predicted kinase activities and differential phosphatase inactivation on wild-type and mutated RAF isoforms.

1.8 DiRas3

The mechanisms and components influencing RAF activation and RAF activity are widely studied, however, still not fully understood. Also very little is known about the regulation of MEK, the only physiologically validated substrate of RAF kinases and best candidate to specifically regulate ERK activity. One candidate that may negatively regulate RAF-MEK-ERK signaling is the Ras-like GTP binding protein DiRas3 (also called ARHI or Noey2). It was found to inhibit epidermal growth factor (EGF) but not phorbol 12-myristate 13-acetate (PMA) mediated phosphorylation of ERK (Luo et al., 2003) and could therefore be involved in the RAF signaling pathway. DiRas3 is encoded by a maternally imprinted tumor suppressor gene and expressed in human ovarian and breast tissue (Hisatomi et al., 2002; Lu et al., 2006; Rosen et al., 2004; Wang et al., 2003; Yu et al., 2005, 1999). In cells, DiRas3 is predominantly GTP-bound.

Expression of DiRas3 reduces cell proliferation, which is accompanied by

Signal	Response
Transient/intensive	Proliferation (Marshall, 1995; Wixler et al., 1996; Tombes et al., 1998)
Sustained/intensive	Cell cycle arrest, differentiation (Marshall, 1995; Wixler et al., 1996; Sewing et al., 1997; Woods et al., 1997; Kerkhoff and Rapp, 1998; Tombes et al., 1998)
Transient/low	Survival
Sustained/low	Transformation (Kerkhoff and Rapp, 1997, 1998)

Table 1.2: **Cellular signals and responses.** The mitogenic signaling pathway can induce different cellular responses depending on its intensity and duration.

the downregulation of the cyclin D1 promoter (Luo et al., 2003; Yu et al., 1999). This function is barely nucleotide dependent supporting the assumption, that its expression is regulated like in the Rnd group of permanent GTP bound proteins (Chardin, 2003). The N-terminal 34 amino acids do not exhibit significant sequence homology to any other proteins and are required for the anti-proliferative effect of DiRas3 (Luo et al., 2003). The molecular mechanisms by which DiRas3 exerts its functions are not known yet.

In this thesis we provide a molecular explanation of how DiRas3 acts as tumor suppressor. We demonstrate that Di-Ras3 is tethered via N- and C-terminal residues to the plasma membrane. At the plasma membrane it binds to activated C-RAF. Ras binding to C-RAF is cooperative with DiRas3 but not *vice versa* (Beck, Robubi et al.–submitted). Unexpectedly, binding of DiRas3 to C-RAF does not affect its kinase activity. However, DiRas3 binds and inhibits MEK. Thus, DiRas3 represents the first Ras-like GTP binding protein directly inhibiting MEK and therefore suppressing ERK phosphorylation. DiRas3 expression has been shown to be controlled transcriptionally via DNA methylation and histon deacetylase complexes as well as posttranscriptionally (Feng et al., 2007; Lu et al., 2006). Our data now suggest, that C-RAF functions as an “and” gate integrating at least two GTPase signaling inputs leading to a block of the RAF signaling cascade at the level of MEK. As the nucleotide binding state of DiRas3 did not influence its binding to C-RAF, we propose that the regulation of the Ras-RAF-MEK-ERK cascade might occur at the level of DiRas3 expression.

Chapter 2

Materials and Methods

2.1 Compound characterization

IR spectra, recorded as ATR, were obtained by using a Biorad PharmalyzIR FT-IR spectrometer. 400-MHz ^1H and 100-MHz ^{13}C -NMR spectra were determined on a Bruker AV-400 spectrometer.

2.2 Cell culture

2.2.1 Conditions for inhibitor studies

NIH 3T3 cells were transformed with constitutively active Gag-v-RAF using the EH^{neo} plasmid (Rennefahrt et al., 2002; Heidecker et al., 1992). The cells were cultured in Dulbecco's modified Eagle's medium (DMEM) supplemented with 10% heat-inactivated fetal calf serum (FCS) and with 2 mM L-glutamine and 100 units/ml penicillin/streptomycin. Cells were cultured at 37 °C in humidified air containing 5% CO_2 . The C-RAF $^{-/-}$ and B-RAF $^{-/-}$ cells (Zhong et al., 2001) were cultured using the same protocol. After inhibitor treatment, the cells were washed once in phosphate-buffered saline (PBS) and then lysed for 10 min on ice in RIPA buffer (25 mM Tris-HCl pH 7.6, 150 mM NaCl, 1% NP-40, 1% sodium deoxycholate, 0.1% SDS, and common protease inhibitors). Subsequently, cells were centrifuged for 10 min at 20000 \times g and 4 °C. The supernatant was subjected to immono blot analysis.

2.2.2 Conditions used for modeling studies

HEK293 and HepG2 cells were cultured in Dulbecco's modified Eagle medium (DMEM) supplemented with 10% heat-inactivated fetal calf serum (FCS).

PC12 cells were also grown in DMEM, but supplemented with 5% FCS and 10% heat-inactivated horse serum (HS). HeLa cells and the human melanoma cell line IF6 were maintained in RPMI 1640 medium with 10% FCS. In addition, all media were supplemented with 2 mM L-glutamine and 100 units/ml penicillin/streptomycin. Cells were cultured at 37 °C in humidified air containing 5% CO₂. Cells were washed once in ice-cold phosphate-buffered saline (PBS) and then lysed for 5 min on ice in 50 mM Hepes (pH 7.8), 0.32 M sucrose, 0.6% Nonidet P-40, 100 mM KCl, 20 mM NaCl, 20 mM iodoacetamide and common protease inhibitors. Subsequently, cells were centrifuged for 5 min at 1000 ×g and 4 °C. The post-nuclear supernatant (PNS) was collected and analyzed by immuno blotting.

2.3 Immuno blot analysis

Protein concentration was assessed using the Pierce BCA-Kit and equal amounts of protein (25 µg) were separated by SDS-PAGE and transferred to nitrocellulose. The blots were blocked for one hour in TBST (Tris-Buffered Saline with Tween-20) supplemented with 5% non-fat milk. They were subsequently incubated over night at 4 °C in primary antibody, namely anti-penta-His (Quiagen), anti-phospho-MEK (CellSignalling), anti-phospho-ERK (#9106, New England Biolabs), and anti-ERK (K23, Santa Cruz Biotechnology). After washing, blots were incubated with secondary antibodies and then detected using the enhanced chemi-luminescence (ECL) detection system (Amersham).

2.4 Kinase assay (immuno blot)

For the production of recombinant RAF kinases, Sf9 cells were infected with baculoviruses at a multiplicity of infection of 5 and incubated for 48 h at 30 °C. The cells were then washed with PBS and pelleted at 230 ×g. The Sf9 cell pellets (2×10^8 cells) were lysed in 10 ml of Nonidet P-40 lysis buffer containing 25 mM Tris-HCl, pH 7.6, 150 mM NaCl, 10 mM Na-pyrophosphate, 25 mM β-glycerophosphate, 25 mM NaF, 10% glycerol, 0.75% Nonidet P-40, and common proteinase inhibitors for 45 min with gentle rotation at 4 °C. The lysate was centrifuged at 27000 ×g for 30 min at 4 °C. The supernatants (10 ml) containing GST-tagged RAF kinases were incubated with 0.5 ml of GS beads (Amersham) for 2 h at 4 °C with rotation. After incubation, the GS beads were washed three times with Nonidet P-40 buffer, with the third wash containing only 0.2% Nonidet P-40 instead of 0.75%. The RAF kinases

bound to the beads were eluted three times with 0.5 ml of 25 mM Tris-HCl, pH 7.6, 150 mM NaCl, 25 mM β -glycerophosphate, 25 mM NaF, 10% glycerol, 0.1% Nonidet P-40, and 20 mM glutathione. The purification procedure for His-tagged RAF kinases was similar to that described above, with the exception that the Sf9 cell lysates (10 ml) were incubated with 0.5 ml of Ni-NTA-agarose. The bound proteins were then eluted with imidazole using a step gradient. The purity of the RAF kinase preparations was documented by SDS-polyacrylamide gel electrophoresis (10% gels) and staining with Coomassie blue (gels not shown). Kinase assays with RAF proteins were performed using recombinant MEK-1 and ERK-2 as substrates in 25 mM Hepes, pH 7.6, 150 mM NaCl, 25 mM β -glycerophosphate, 10 mM MgCl_2 , 1 mM dithiothreitol, and 1 mM sodium ortho vanadate buffer (50 ml final volume). Following additions of purified RAF kinases (5–10 ml) and ATP (500 μM), the samples were incubated for 30 min at 26 °C. The incubation was terminated by the addition of Lämmli sample buffer, and the proteins were separated by 10% SDS-PAGE and transferred to nitrocellulose membranes. The extent of ERK phosphorylation was determined by anti-phospho-ERK antibodies (#9106, New England Biolabs) and detected using an enhanced chemiluminescence (ECL) detection system (Amersham).

2.5 Kinase assay (ELISA)

The inhibitors were dissolved in DMSO. The mitogenic signaling pathway was reconstructed using GST-C-RAF-Y340D/Y341D or His-B-RAF expressed in Sf9 insect cells, GST-MEK-1 expressed in *E. coli*, and His-ERK-2 expressed in *E. coli*. The reaction mixture (1 mM ATP, 10 mM MgCl_2 , 150 mM NaCl, 25 mM β -glycerophosphate, 25 mM Hepes, pH 7.5 and 20–150 ng MEK, ERK and RAF respectively) was pre-incubated with the inhibitors for 30 minutes at ambient temperature. The kinase reaction was started by uniting the pre-incubated kinases (50 μl final volume) and stirring at 26 °C for 30 minutes. The reaction was terminated by addition of SDS (2% final concentration) and heating (50 °C, 10 min). 96 well micro titer plates (MTPs), coated with anti-ERK antibodies (K-23, Santa Cruz Biotechnology), were incubated with the reaction mixture (60 min) and subsequently washed three times with TBST (25 mM Tris, 140 mM NaCl, 3 mM KCl, 0.05% Tween-20, pH 7.4). The MTPs were incubated with anti-phospho-ERK antibody (#9106, New England Biolabs, 1:500, 1% BSA, TBST) at 4 °C over night and washed three times with TBST. Subsequently the MTPs were incubated with IgG^{POD} conjugated secondary mouse antibody (#NA931, Pharmacia, 1:2500, 1 h) and washed three times with TBST. The phospho-ERK levels were mea-

sured colorimetrically in an ELISA reader at 492 nm after incubation with o-phenylenediamine hydrochloride (OPD) buffer (37 °C, 30 min, 50 μ l).

2.6 Kinase assay (DiRas3)

Kinase activity assays were performed as described in Kinase assay (immuno blot) using purified MEK-1-His₆ and His₆-ERK as substrates in 25 mM Hepes, pH 8.0, 150 mM NaCl, 25 mM β -glycerophosphate, 10 mM MgCl₂, and 1 mM sodium vanadate buffer (50 μ l final volume). Following additions of purified GST-C-RAF-Y340D/Y341D kinase (0.5 μ g) and increasing amounts of purified His₆-DiRas3 or His₆- Δ N-DiRas3 and ATP (1 mM) the mixtures were incubated at 30 °C for 20 min. The incubation was terminated by addition of SDS loading buffer and boiling at 96 °C for 5 min. The samples were applied to SDS-PAGE, blotted and stained against pMEK and pERK. To obtain an active MEK preparation purified GST-MEK-1 isolated from *E. coli* was incubated with purified His-B-RAF for 50 min at 27 °C in 25 mM Hepes, pH 8.0, 150 mM NaCl, 25 mM β -glycerophosphate, 10 mM MgCl₂ buffer and 1 mM ATP. The phosphorylated and active GST-MEK-1 was subsequently separated from B-RAF using GSH-Sepharose.

2.7 Biosensor measurements

The biosensor measurements were carried out either on a BIAcore-J system (Biacore AB, Uppsala, Sweden) at 25 °C. To measure DiRas3-RAF interactions the biosensor chip CM5 was loaded with anti-GST antibody using covalent derivatization according to the manufacturer's instructions. The GST-tagged C-RAF and C-RAF mutants were expressed in Sf9 insect cells and purified as described in Hekman et al. (2002). These C-RAF preparations were immobilized in biosensor buffer (10 mM Hepes, pH 7.4, 150 mM NaCl and 0.01% NP-40) at a flow rate of 10 ml/min, which resulted in a deposition of approximately 800–1200 response units (RU). Next purified DiRas3-GDP was injected. The unspecific binding was measured in the reference cell and subtracted.

2.8 Mass spectrometry measurements

GST-tagged C-RAF-Y340D/Y341D was expressed in Sf9 cells, partially purified (Robubi et al., 2005), treated with compound **1** (100 μ M, 60 min, 30 °C) and applied to SDS-PAGE (5 pmol). Proteins were visualized by subsequent

Coomassie Blue applying the method described in Neuhoff et al. (1988). In-gel reduction, acetamidation and tryptic digestion were done according to Wilm et al. (1996). After elution of the peptides, solutions were desalted using Millipore C18 ZipTip according to the manufacturers instructions. ESI-MS was performed on a Bruker APEX II FT-ICR mass spectrometer (Bruker Daltonic GmbH Bremen).

2.9 Gel filtration

His-tagged C-RAF and His-tagged B-RAF were coexpressed in Sf9 insect cells. The cells were treated with inhibitors for 30 minutes and subsequently lysed for 30 minutes at 4 °C in lysis buffer (25 mM Tris, 150 mM NaCl, 15% glycerol, 1% Chaps, 25 mM NaF, 25 mM β -glycerophosphate, 0.1% β -mercaptoethanol, and common protease inhibitors, pH 7.4). The lysate was directly subjected to gel filtration chromatography (Äkta Explorer 100, Superdex 200, 25 mM Tris, 150 mM NaCl, 15% glycerol, pH 7.4) after centrifugation (20000 \times g, 30 min, 4 °C). Runs with thyroglobulin (670 kD) and aldolase (158 kD) were used as standards. The proteins were collected in fractions of equal volume (1 ml) and precipitated with trichloroacetic acid (TCA). The precipitated proteins were solved in Lämmli buffer and subjected to immuno blot analysis.

2.10 Bioinformatics

2.10.1 Molecular modeling

The crystal structures of active Lck (Zhu et al., 1999) and p38 MAP kinase in complex with diphenyl urea inhibitors (Pargellis et al., 2002) were used to model the structure of the kinase domain of B-RAF in complex with BAY 43-9006. The coordinates of the activation segment were taken from the kinase domain of the insulin receptor with the DFG amino acid motif in the “DFG-out” conformation, as in the p38 MAP kinase structure (Hubbard et al., 1994). The PDB coordinate file of Lck required some editing in a standard text browser in order to be accepted by the MODELLER package. In particular, the phosphorylated tyrosines and serines are unknown to MODELLER and had to be replaced by unphosphorylated versions of these amino acids. The sequences were aligned manually using Seaview. Alignments were adjusted in a standard text editor. The model was generated with MODELLER (Sali and Blundell, 1993) based on the alignment using the standard parameter setting of the MODELLER package. The inhibitor molecules were included as block residues (BLK).

2.10.2 Dynamic pathway modeling

For calculation of the kinase-phosphatase cascade, the formalism given in Equation 3.1 on page 51 was applied. Several assumptions for simplified modeling were used, in particular, first-order rate constants allowed the concise formula given to be obtained. The Matlab software library was obtained from MathWorks Inc. A custom written program with different subroutines first solved the set of four ordinary differential equations (ODEs) summarized in Figure 3.11 and next plotted different parameter settings and values, as described in the Results. Calculations took between seconds and several minutes on a PC with a Pentium 4 processor, depending on the time frame calculated and the convergence of the ODE set according to the parameter set used. Concentrations of Ras, RAF, MEK and ERK in Figure 3.12 were set at 1, 10, 20 and 30, respectively. Concentrations for Figure 3.13 were according to experimental data and set at $C_{Ras} = 33$, $C_{RAF} = 17$, $C_{MEK} = 1300$ and $C_{ERK} = 1250$ (concentrations according to Ferrell (1996)).

For the activity values in Figure 3.12, all cascade members were modeled to be active with $\alpha_{RAF} = 0.1$, $\alpha_{MEK} = 1$, $\alpha_{ERK} = 5$, $\beta_{RAF} = 0.5$, $\beta_{MEK} = 0.5$, $\beta_{ERK} = 1$, $C_{Ras} = 1$, $C_{RAF} = 10$, $C_{MEK} = 20$, $C_{ERK} = 30$, and $\lambda = 1$. In Figure 3.13 (page 54), we systematically varied activation and dephosphorylation parameters and then solved the set of differential equations. Figure A.1 (page 94) shows plots for the following RAF-specific settings: B-RAF $\alpha_1 = 1, 80, 1000, 50000$, $\beta_1 = 8$; C-RAF $\alpha_1 = 1, 80, 1000, 50000$, $\beta_1 = 70$. For the other proteins (Ras, ERK and MEK), activation and phosphorylation was set at $\lambda = 0.069$ (Ras receptor-module activation half-life of 600 s) for the Ras-GTP receptor module decay, and activation of $\alpha_{MEK} = 600$, $\alpha_{ERK} = 600$, with dephosphorylation at $\beta_{MEK} = 170$ and $\beta_{ERK} = 170$. Parameter settings for time were systematically varied between 30 s and 3 h.

Chapter 3

Results

3.1 Development of a novel RAF kinase inhibitor

3.1.1 Homology modeling

The crystal structures of active Lck (Zhu et al., 1999) and p38 MAP kinase in complex with diphenyl urea inhibitors (Pargellis et al., 2002) were used to model the structure of the kinase domain of B-RAF in complex with BAY 43-9006. The coordinates of the activation segment were taken from the kinase domain of the insulin receptor (Hubbard et al., 1994) with the DFG amino acid motif in the “DFG-out” conformation, as in the p38 MAP kinase structure. The sequences were aligned manually and the model was generated with MODELLER (Sali and Blundell, 1993). The crystal structure published later (Wan et al., 2004), was strikingly similar to our model but has an unresolved activation segment. A look at the PDB entry (1UWH) showed that the crystal structures of Lck and p38 MAP kinase were used for the refinement. Our homology model revealed, the close proximity of the pyridine moiety of the bound BAY 43-9006 molecule and the cysteine 532 residue (Cys109 in p38 α). This residue is situated at the hinge region of the kinase domain between the small n-lobe and the large c-lobe (Figure 3.1A).

We designed the structure of compound **1** (Figure 3.1B). The diphenyl moiety was used to mimic BAY 43-9006 and the epoxy moiety was introduced in order to provide a mild electrophilic group for the nucleophilic sulfur atom of the Cys532 residue to react with (Figure 3.2). The molecular modeling coordinate file of compound **1** in complex with the kinase domain of B-RAF is deposited in Appendix A. The nucleophilic attack would open the tight ring system of the epoxide and thus irreversibly link **1** to the protein

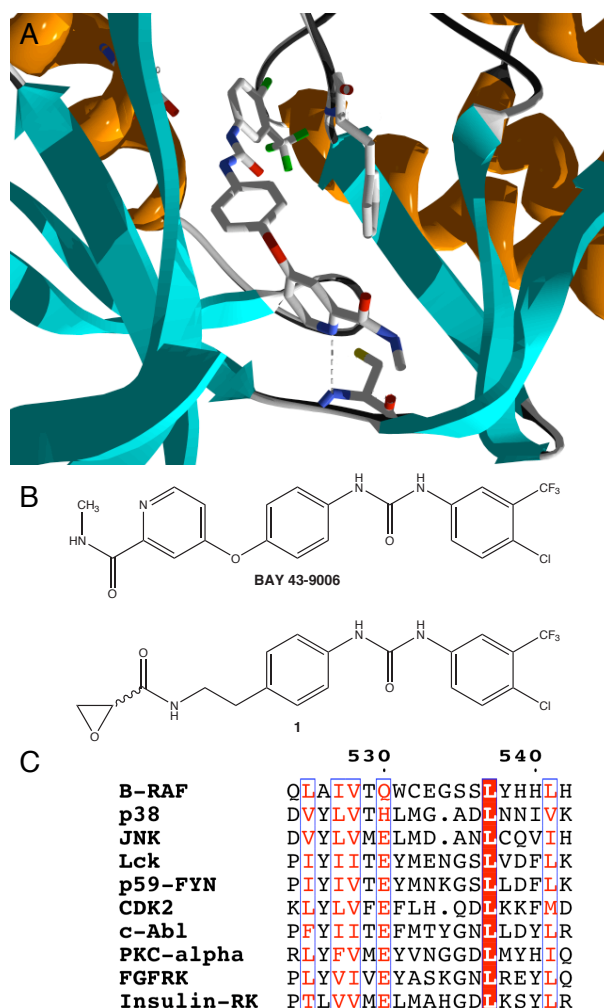


Figure 3.1: **Development of a new lead compound.** **A:** Homology model of BAY 43-9006 (stick model) in complex with B-RAF (ribbons). All β -strands are shown in blue, α -helices are shown in orange. The pyridine residue of the BAY 43-9006 molecule forms a hydrogen bond with a conserved cysteine residue in the hinge region of the RAF kinase. Our model fits well to crystallographic data Wan et al. (2004). **B:** Structure of BAY 43-9006 and compound **1**. The diphenyl urea moiety (right) is preserved while the pyridine moiety is replaced by an epoxide group (left). **C:** Alignment of the hinge region of different kinases. The leucine residue 537 is strictly conserved and shown in a red box with white lettering. Similar residues are boxed and shown with red lettering. The dots show gaps. The cysteine 532 residue is present in all mammalian RAF kinases but not in most other protein kinase families.

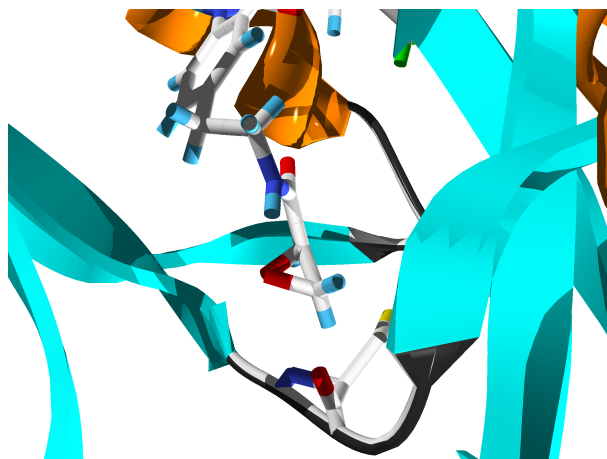


Figure 3.2: **Model of compound 1 in complex with B-RAF.** Homology model of compound **1** (stick model) in complex with B-RAF (ribbons). All β -strands are shown in blue, α -helices are shown in orange. The epoxide residue of the compound **1** molecule forms a hydrogen bond with a conserved cysteine residue in the hinge region of the RAF kinase. The orientation of the epoxide moiety relative to the nucleophilic sulfur atom of the Cys532 residue is crucial: the sulfur atom needs to attack the epoxide group from the back of the beta carbon.

(Figure 4.1). Previously CI-1033, an irreversible pan-erbB inhibitor, was developed successfully in the same manner. Apart from inhibiting the receptor tyrosine kinase activity, the covalent modification also proved to increase the degradation of the protein (Fry, 2003). Additionally, irreversible inhibitors are generally better suited to provide prolonged suppression of signaling pathways (Allen et al., 2002) and are in principle less sensitive to multi drug resistance (MDR). However it should be noted that the cysteine residue in the hinge region of the RAF kinases has a different position compared to the cysteine residue in the erbB receptor tyrosine kinases to which CI-1033 is targeted. We were therefore dealing with a truly novel system.

Cys532 is conserved throughout all mammalian RAF kinase isoforms (A-, B-, and C-RAF) but is found in few other protein kinases (Figure 3.1C). Thus we were expecting compound **1** to possess high specificity and, due to the fact that an epoxide is an relatively mild electrophile, low toxicity.

Synthesis of **N**-(2-{4-[(4-chloro-3-(trifluoromethyl)phenyl)amino]carbonyl}amino]phenyl)ethyl)oxirane-2-carboxamide (**1**). All steps are depicted in Figure 3.3.

(a) KBr (20 g), D/L-serine (**2**) (5.25 g, 50 mmol) and HBr (62%), (13.7 g) were dissolved in H₂O (50 ml). A solution of NaNO₂ (3.8 g, 55 mmol) in

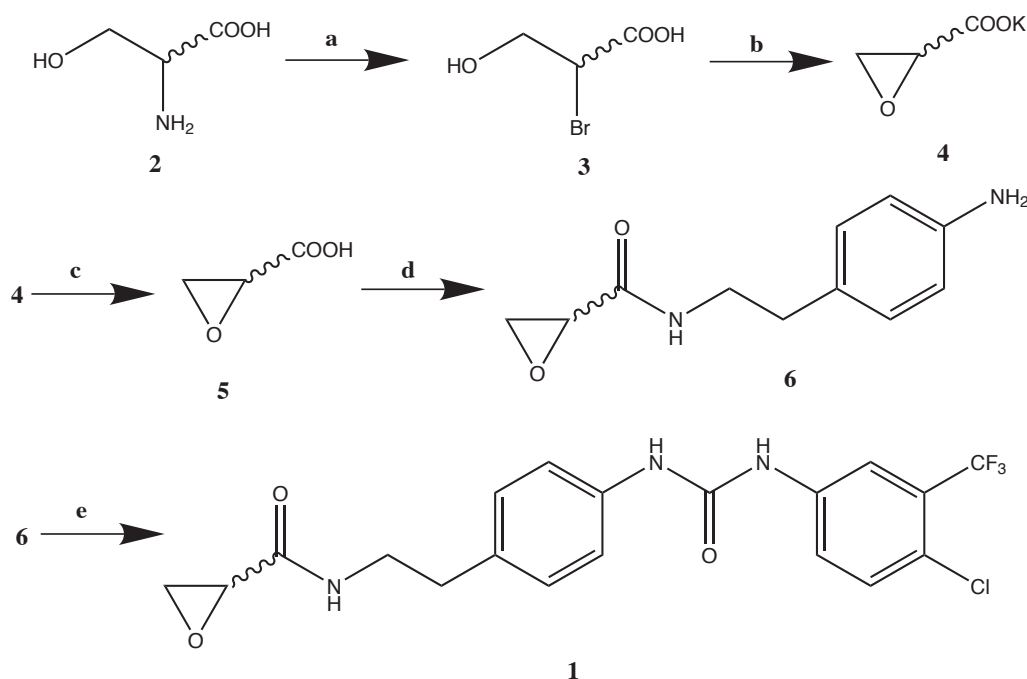


Figure 3.3: **Synthesis of compound 1.** The synthesis route is briefly sketched. The reaction conditions were: (a) H_2O , KBr, HBr, NaNO_2 , -15°C ; (b) MeOH, KOH (2 eq), -50°C ; (c) Ion exchange (Dowex 50Wx2) and lyophilization; (d) THF, 4-methyl-morpholine, isobutyl chloroformate, 2-(4-aminophenyl)ethylamine, -15°C ; (e) CH_2Cl_2 , 4-chloro-3-(trifluoromethyl)phenyl isocyanate, 0°C . Details are given in the text.

H_2O (20 ml) was added dropwise (1 h) at -15°C with stirring. The reaction mixture was further stirred over night and then extracted seven times with Et_2O (50 ml). The combined organic extracts were dried over Na_2SO_4 , filtered and the solvent was removed *in vacuo*. Yield: 94%, 7.975 g R/S-2-Bromo-3-hydroxy-propionic-acid (**3**) as a yellow oil (Grosjean et al., 1994). ^1H NMR (CDCl_3): δ (ppm) = 4.35 (dd, $J = 5.3, 7.3\text{ Hz}$, 1H), 4.0 (ddd, $J = 6.3, 12.1, 17.3\text{ Hz}$, 2H). ^{13}C NMR (CDCl_3): δ (ppm) = 171.8, 63.9, 44.6.

(b) R/S-2-Bromo-3-hydroxy-propionic-acid (**3**) (7.63 g, 45 mmol) was dissolved in MeOH (60 ml) and cooled to -50°C . KOH (5.12 g, 90 mmol, 2 eq) dissolved in MeOH (35 ml) was added dropwise (45 min). The pH of the solution became neutral, after stirring for three hours at room temperature. Then the solvent was removed *in vacuo* and the potassium salts were precipitated by adding Et_2O (150 ml) and stirring for one hour. The salt cake was removed by suction and heated with EtOH (100 ml) under reflux. After hot

filtration the potassium-oxiranyl carboxylate precipitated when the solution was cooled to room temperature and further cooling over night at -30°C . Yield 3.3 g potassium-oxiranyl carboxylate (**4**) Grosjean et al. (1994). ^1H NMR (D_2O): δ (ppm) = 3.4 (dd, $J = 2.8, 4.7\text{ Hz}$, 1H), 2.9 (m, 2H). ^{13}C NMR (D_2O): δ (ppm) = 171.8, 64, 44.6, 176.7, 49.5, 46.0. Anal. ($\text{C}_3\text{H}_3\text{O}_3\text{K}$) C: calcd, 28.57; found 26.21, H: calcd, 2.38; found 2.88.

(c) Potassium-oxiranyl carboxylate (3.3 g, 26 mmol) was dissolved in H_2O (20 ml) and subjected to ion exchange chromatography on an acidic stationary phase (Dowex 50Wx2). The free acid (**5**) was obtained by subsequent freeze drying over night as a yellow oil (1.93 g, 18.3 mmol, 70% yield). ^{13}C NMR (D_2O) δ (ppm) = 173.6, 47.7, 46.6.

(d) Compound **4** (212 mg, 2 mmol) was solved in abs. THF (10 ml) and cooled to -15°C . Then 4-methyl-morpholine (202 mg, 2 mmol), isobutyl chloroformate (273 mg, 2 mmol) and 2-(4-aminophenyl)ethylamine (272 mg, 2 mmol) were added and the mixture was stirred for thirty minutes at -15°C . The mixture was allowed to warm to r.t. and the precipitate was removed by filtration and washed with THF. The THF was partially removed *in vacuo* and CH_2Cl_2 (25 ml) was added and the solution was extracted two times with 15 ml phosphate buffer (pH 7). The organic phase was dried over Na_2SO_4 , filtered and used directly for the next step.

(e) 4-Chloro-3-(trifluoromethyl)phenyl isocyanate (200 mg, 1 mmol) was added to the organic phase with stirring (0°C , 30 min). The product (50 mg; 11% yield) readily precipitated from the solution and was removed by suction and dried. ^1H NMR (DMSO-d_6) δ (ppm) = 9.1 (s, 1H), 8.7 (s, 1H), 8.11 (s, 1H), 8.09 (m, 1H), 7.6 (m, 2H), 7.4 (d, $J = 8.4\text{ Hz}$, 2H), 7.1 (d, $J = 8.4\text{ Hz}$, 2H), 3.3 (m, 3H), 2.8 (m, 4H). ^{13}C NMR (DMSO-d_6) δ (ppm) = 167.6, 152.4, 139.4, 137.3, 133.1, 131.9, 128.9, 126.7 (CF_3), 122.9, 118.7, 48.5, 45.6, 39.9, 34.2. IR $\nu\text{ cm}^{-1}$ 1655, 1596, 1542, 1515, 1484, 1416, 1310, 1258, 1227, 1175, 1129, 1032, 888, 828, 685, 662. Anal. ($\text{C}_{19}\text{H}_{17}\text{N}_3\text{O}_3\text{ClF}_3$) H: C: calcd, 53.34; found, 51.32, N: calcd, 9.82; found, 9.20.

3.1.2 Activity of compound **1** *in vitro*

Compound **1** showed inhibitory activity toward B-RAF and C-RAF *in vitro* that was lower compared to BAY 43-9006 as shown in Figure 3.4 and Table 3.1. In addition, we did not detect that **1** was an irreversible inhibitor in time kinetics experiments suggesting a very slow reaction rate (see Figure 3.5). To detect very low levels of modified protein, we performed mass spectrometric measurements of the RAF protein, pre-incubated with **1**.

Mass spectrometry: GST-C-RAF-Y340D/Y341D was digested with trypsin after, respectively without pretreatment with compound **1** (100 μM , 50 min,

30 °C). The resulting peptides were used for mass spectrometric analysis. The ratio of the signal intensities corresponding to peptides containing cysteine 657 (corresponding to Cys532 in B-RAF) and other peptides was comparable in both samples (Figure 3.6), indicating that at least the major amount of protein was not covalently modified at cysteine 657. Furthermore, no signal corresponding to compound **1** linked by a thioether bonding with a peptide containing cysteine 657 could be detected. Our results indicate that no significant covalent binding occurs between **1** and the protein.

3.1.3 Activation in cell culture

A striking observation was made in cell culture experiments. NIH 3T3 fibroblasts transformed by constitutively active RAF were treated with compound **1**. The transformed phenotype was not reversed (data not shown). Examination of pERK levels revealed that the mitogenic signaling pathway was actually

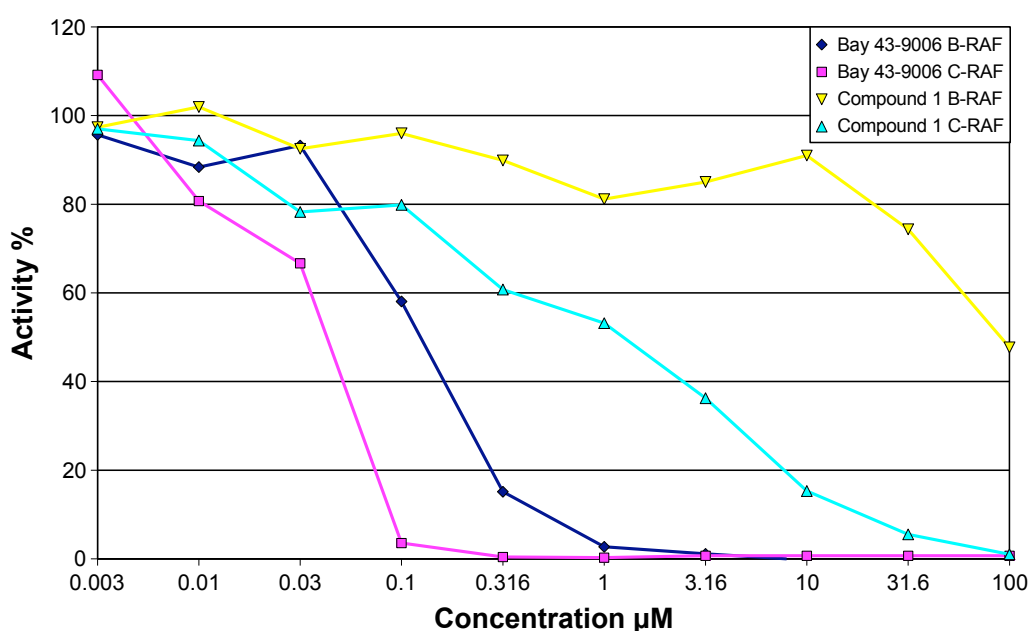


Figure 3.4: **Inhibition of RAF kinases in an *in vitro* kinase assay.** The plot depicts inhibition of B-RAF and C-RAF by compound **1** and BAY 43-9006 *in vitro* using a coupled Raf/MEK/ERK ELISA assay. The kinase activity relative to the DMSO control is plotted against the concentration of the inhibitors. BAY 43-9006 possesses higher potency than **1**. However, the IC_{50} values we measured, were considerable higher than described in the literature. The assay was repeated three times and gave highly reproducible results.

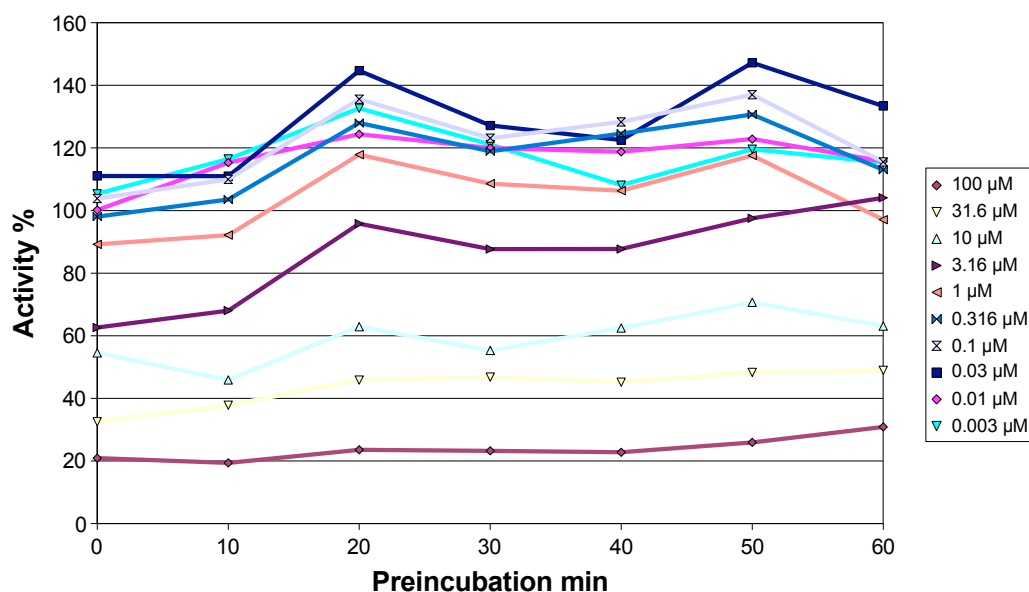


Figure 3.5: **Time kinetics experiment.** Performed to distinguish reversible from irreversible inhibition. C-RAF was pre-incubated with compound **1** at room temperature for a variable amount of time (x-axis). Subsequently, ATP was added and the kinase activity was detected as described in Materials and Methods. An irreversible inhibitor would show enhanced inhibition (y-axis) when it is given more time to react to the protein. Compound **1** did not show any increased activity at any concentration (different graphs) when the pre-incubation time was increased.

up-regulated after treatment with the inhibitor. The activation was profound (Figure 3.7A) and rapid (Figure 3.7B). The counter-intuitive activation of the RAF signaling pathway in cell culture was already described for other RAF kinase inhibitors such as ZM 336372 (Hall-Jackson et al., 1999a), GW 5074 (Lackey et al., 2000; Chin et al., 2004), and SB 203580 (Hall-Jackson et al., 1999b) (Figure 1.5), but the mechanism is unknown.

Dimerization of RAF kinases leads to activation in a Ras-dependent manner (Farrar et al., 1996; Luo et al., 1996; Rushworth et al., 2006). Many oncogenic mutants of B-RAF have impaired kinase activity but nevertheless activate the mitogenic signaling pathway by dimerizing with C-RAF (Wan et al., 2004). Most of these mutations are detected in the glycine rich loop and the activation segment and thus overlap with the inhibitor binding site. Diphenyl urea inhibitors bind to protein kinases in the DFG-out conformation (Pargellis et al., 2002; Wan et al., 2004). The fact that the kinase domain of B-RAF could only be crystallized in the presence of BAY 43-9006 (Wan

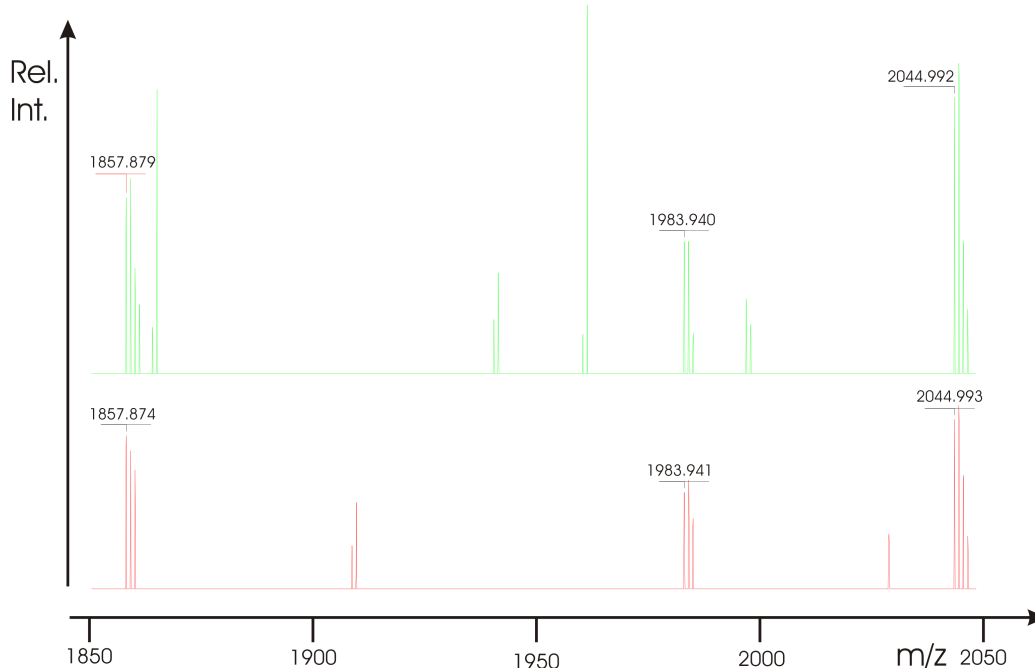


Figure 3.6: **Mass spectrometry data.** This diagram shows the m/z range 1850–2050, obtained from peptide samples generated by tryptic in-gel digestion of GST-C-RAF-Y340D/Y341D after (upper part) respectively without (lower part) pretreatment with compound **1** (100 μ M, 60 min, 30 °C). Peptides with the m/z 1857.87 correspond to AA861–877, peptides with the m/z 2044.99 correspond to AA490–508. Peptides with the m/z 1983,94 correspond to the peptide containing the cysteine corresponding to cysteine 532 (AA648–664).

et al., 2004) is another indication that RAF-RAF interactions are effected by binding to these ligands. We assumed that compound **1** may activate RAF kinases by induction of hetero-dimerization of B- and C-RAF. To test this hypothesis we treated starved mouse embryonal fibroblasts from C-RAF^{-/-} and B-RAF^{-/-} mouse embryos with compound **1**, BAY 43-9006 and ZM 336372. We did not detect a significant activation by compound **1** and BAY 43-9006, indicating that compound **1** indeed activates through the formation of heterodimers (Rushworth et al., 2006). In contrast, activation was observed in the presence of ZM 336372 (Figure 3.8). This may indicate that there are multiple mechanism for paradoxical activation, or that ZM 336372 recruits A-RAF for hetero-oligomerization.

To test for the formation of heterooligomers, we co-expressed His-tagged B-RAF and C-RAF in Sf9 insect cells. The cells were treated with inhibitor for thirty minutes prior to lysis. The lysates were subjected to size exclusion

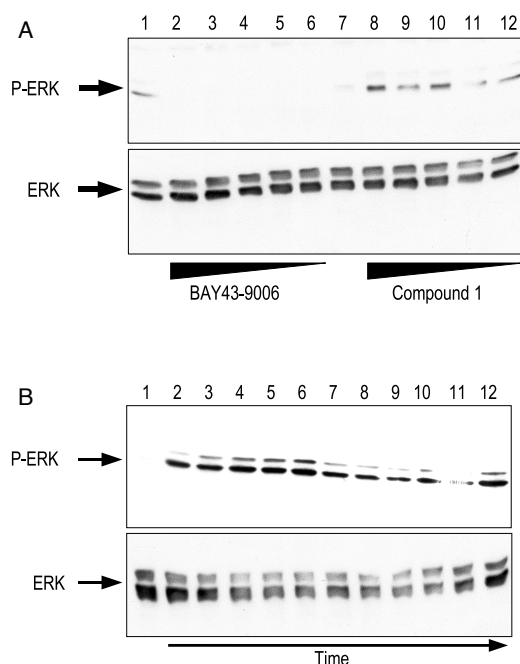


Figure 3.7: **Elevated levels of pERK after treatment with compound 1.** A: Lanes 1 and 7: DMSO controls; lanes 2–6: decreasing concentrations of BAY 43-9006 (10, 8, 6, 4, and 2 μM); lanes 8–12: decreasing concentrations of compound 1 (24, 22, 20, 18, 16 μM). B: pERK levels after different time points. Lane 1: DMSO control; lanes 2–12: 10, 20, 30, 40, 50, 60, 70, 80, 90, 100, 110 min treatment with compound 1 (20 μM).

gel filtration chromatography. The fractions were subjected to SDS-PAGE immuno blotting using an anti-penta-His antibody to detect RAF proteins. We could clearly show that C-RAF elutes only in high mass and the low mass fractions, indicating that it is in a partially oligomerized state. However, addition of inhibitors did not alter the profile (Figure 3.9).

Thus the alternative hypothesis should also be considered: activation by inhibition of an inhibitory kinase in a pathway not active under starvation. In fact, several such kinases would be potential targets for this (Appendix A).

3.1.4 Other compounds

Compound 1 is was the last of several compound which were synthesized and tested in *in vitro* kinase assays.

Synthesis of N-(2{4-([4chloro3(trifluoromethyl)phenyl]amino)-carbonyl)amino]phenyl}ethyl)acrylamide (7).

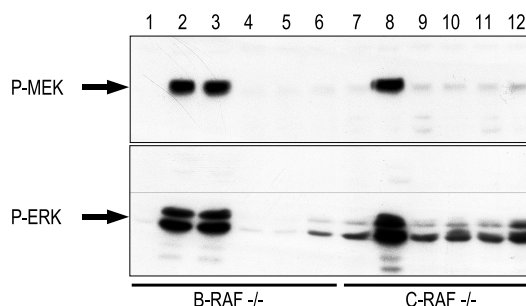


Figure 3.8: **No activation by compound 1 in starved RAF knockout cells.** Mouse embryonal fibroblasts (MEFs) from C-RAF^{-/-} and B-RAF^{-/-} knockout mouse embryos were starved for 42 hours in 0.05% serum prior to treatment with different kinase inhibitors for one hour. Lanes 1 and 7: DMSO controls; lane 2, 3 and 8: stimulation with 20% FCS; lane 6 and 12: ZM 336372 inhibitor (10 μM); lane 5 and 11 compound 1 (20 μM); lane 4, 9, and 10 BAY 43-9006 (800 nM).

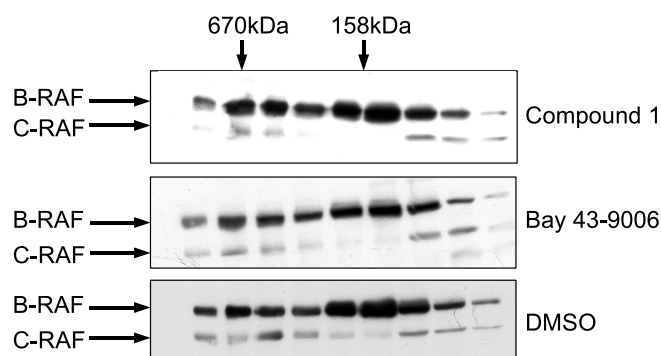


Figure 3.9: **Hetero-oligomerization of B-RAF and C-RAF *in vitro*.** His tagged B- and C-RAF were coexpressed in Sf9 cells and subjected to gel filtration chromatography as described in Experimental Section. The protein standards thyroglobulin (670 kDa) and aldolase (158 kDa) have elution peaks as indicated by the arrows.

(a) 4-Dimethylaminopyridine (DMAP, 9 mg), di-tert-butyl dicarbonate (Boc₂O, 151 mg), triethylamine (111 μl), and acrylic acid (48 μl) were dissolved in CH₂Cl₂ and stirred (30 min) at room temperature. 2-(4-Aminophenyl)ethylamine (**9**) was added and the solution was stirred (3 h) at room temperature. The solution was extracted three times with 10 ml phosphate buffer (pH 7). The organic phase was dried over Na₂SO₄, filtered and the solvent was removed *in vacuo*, gaining **8**.

(b) **8** was dissolved in abs. THF and 4-chloro-3-(trifluoromethyl)phenyl isocyanate (94 mg, 0.42 mmol) was added with stirring (0 °C, 30 min). The product (**7**) readily precipitated from the solution and was separated by suction and dried.

Synthesis of 4-[(**4-Chloro-3-(trifluoromethyl)phenyl**]amino)carbonyl]amino]phenyl acrylate (**10**).

(c) p-Aminophenol (**11**, 5 g, 46 mmol) and di-tert-butyl dicarbonate (Boc₂O, 10 g, 46 mmol) were stirred in THF (18 h) at room temperature. The THF was removed *in vacuo* (**8**).

(d) The potassium salt of **8** (5 mmol) was dissolved in THF and acrylic acid chloride (0.45 g, 5 mmol) was added (−10 °C, 18 h). The solution was filtered and the THF was removed *in vacuo*. **13** was crystallized in isopropanol.

(e) **13** (0.1 g, 0.38 mmol) was dissolved in CH₂Cl₂ and trifluoroacetic acid (TFA, 1.2 eq) was added. After stirring at room temperature (4 d), 10 ml of a saturated Na₂CO₃ solution was added and the two phases were separated. The aqueous solution was extracted two times with CHCl₃, the organic phases were united, dried over NaSO₄, and the solvent was removed *in vacuo* (**14**).

(f) **14** (0.054 g, 0.331 mmol) and 4-chloro-3-(trifluoromethyl)phenyl isocyanate were stirred in Et₂O (1 h) at room temperature. **10** precipitated readily from the reaction mixture. It and was separated by suction and dried.

Inhibition of C-RAF and MEK by **1**, **7**, **10**, and commercial RAF kinase inhibitors is presented in Table 3.1.

3.2 Dynamic modeling

As Table 1.2 on page 30 shows, there are many different cellular responses mediated by RAF in the RAF-MEK-ERK cascade such as proliferation, cell cycle arrest or differentiation, survival and transformation. From a cell biology point of view, these various responses depend on the cellular context. To examine how far these different effects can be mediated by the type of RAF-molecule present, we first did mathematical modeling of the RAF-ERK cascade as shown in Figure 1.2 on page 24. The signaling module consists of several steps (Ras-GTP, RAF, MEK, ERK). Furthermore, there is an intensive interplay between kinases (with specific activities α_i) and phosphatases (with specific activities β_i) as depicted in Figure 3.11. To model these activities we use a formalism introduced by Heinrich et al. (2002). Applied on the mitogenic signaling pathway this leads to a set of differential equations for the activities of each kinase or phosphatase implicated in the pathway according to the summary Equation 3.1.

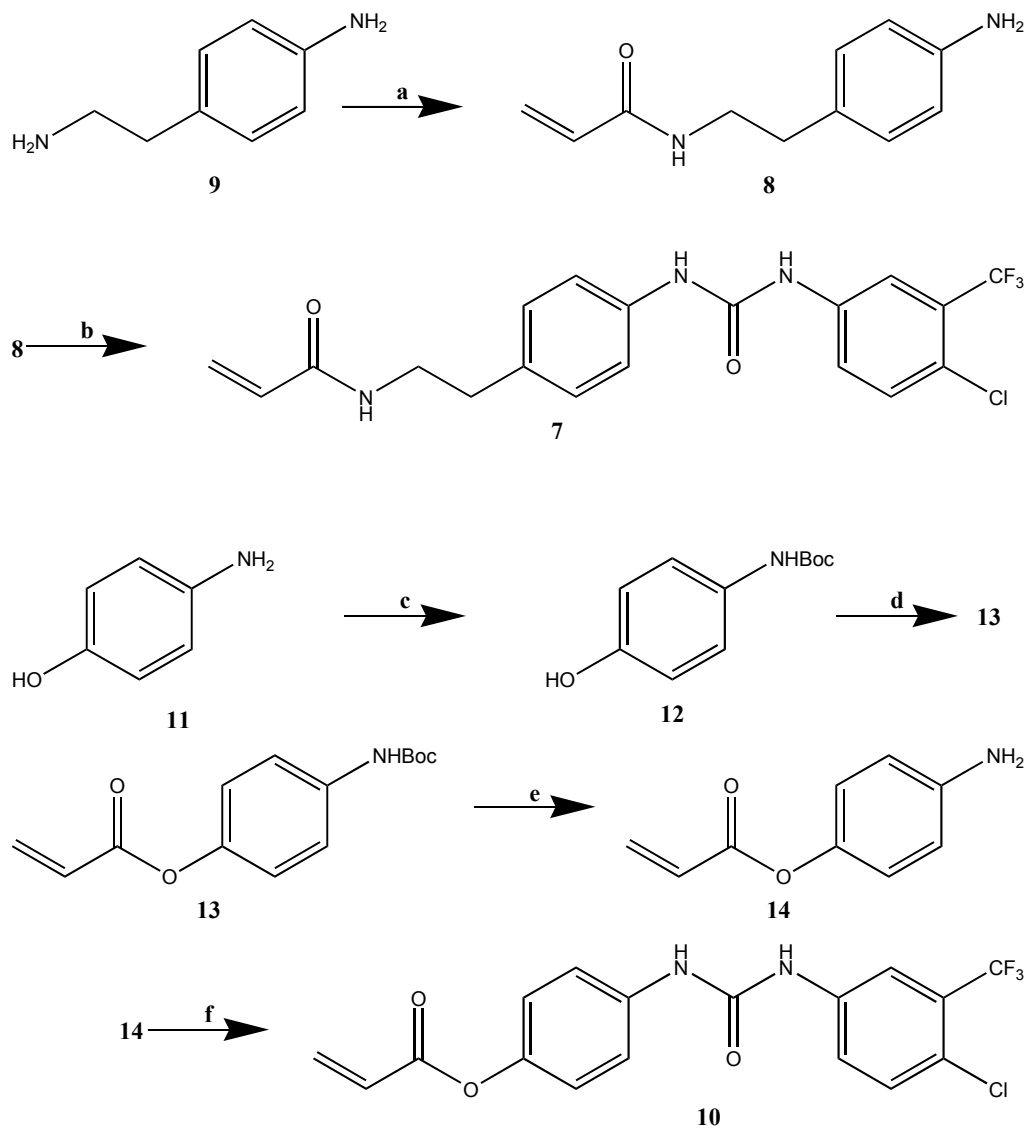


Figure 3.10: **Synthesis of compounds 10 and 16.** The synthesis route is briefly sketched. The reaction conditions were: (a) DMAP, Boc_2O , Et_3N , acrylic acid, CH_2Cl_2 , r.t.; (b) THF, 4-chloro-3-(trifluoromethyl)phenyl isocyanate, 0°C ; (c) p-Aminophenol, Boc_2O , THF, r.t.; (d) Acrylic acid chloride, THF, -10°C ; (e) CF_3COOH , CH_2Cl_2 , r.t.; (f) 4-Chloro-3-(trifluoromethyl)phenyl isocyanate, CH_2Cl_2 , r.t. Details are given in the text.

Conc.	1	7	10	BAY ...	ZM ...	GW ...	1 *	7 *	10 *
3 nM	97	100	119	140	107	88	111	104	86
10 nM	95	105	117	137	99	83	100	96	93
33 nM	79	91	99	81	74	58	108	90	91
100 nM	81	96	104	4	51	44	87	91	95
333 nM	63	86	117	4	17	33	87	93	97
1 μ M	56	70	111	4	8	14	106	73	98
3.3 μ M	40	63	100	3	4	3	95	77	99
10 μ M	20	53	76	4	3	2	97	79	98
33 μ M	11	50	49	3	3	3	78	70	82
100 μ M	6	19	14	4	3	2	25	48	23

Table 3.1: **Inhibition of C-RAF and MEK by different inhibitors *in vitro*.** Compounds **1**, **7**, and **10** inhibit ERK phosphorylation in the a coupled C-RAF-MEK-ERK ELISA assay. The inhibitory activity of **7** and **10** is very low compared to the commercial RAF kinase inhibitors BAY 43-9006 (BAY ...), ZM 336372 (ZM ...), and GW 5074 (GW ...) (Figure 1.5, p. 28) and also compared to **1** (Figure 3.1, p. 40). The same activity is detected in an MEK-ERK kinase assay (*), indicating that **7** and **10** do not show any significant binding to RAF kinases. However, **1** clearly shows inhibition—and thus binding—to C-RAF.

$$\frac{dX_i}{dt} = \alpha_i X_{i-1} \left(1 - \frac{X_i}{C_i}\right) - \beta_i X_i. \quad (3.1)$$

Although there are a number of components involved, modeling using Matlab (MathWorks Inc. Natick, MA) to solve the set of differential equations summarized by the formula in Equation 3.1 shows for standard parameters that the basic function of the cascade is signal amplification: an input signal activates the Ras receptor module (assumed to be one module for simplicity) with an exponential decay. Subsequent peaks of RAF, MEK and ERK follow each other with some time delay (time in arbitrary units) and the signal peak is augmented throughout the cascade (Figure 3.12).

However, this standard behavior does not yet explain the complex differential responses known from cell biology studies (Table 1.2). We reasoned that the different isoforms of RAF, in particular B-RAF and C-RAF, are central for the differential responses mediated by the cascade. In particular, there are indications for differences in their dephosphorylation and activation in the RAF-ERK cascade. For example, data (Lew, 2003) for ERK show that for each phosphorylation step the activity increases in a specific manner

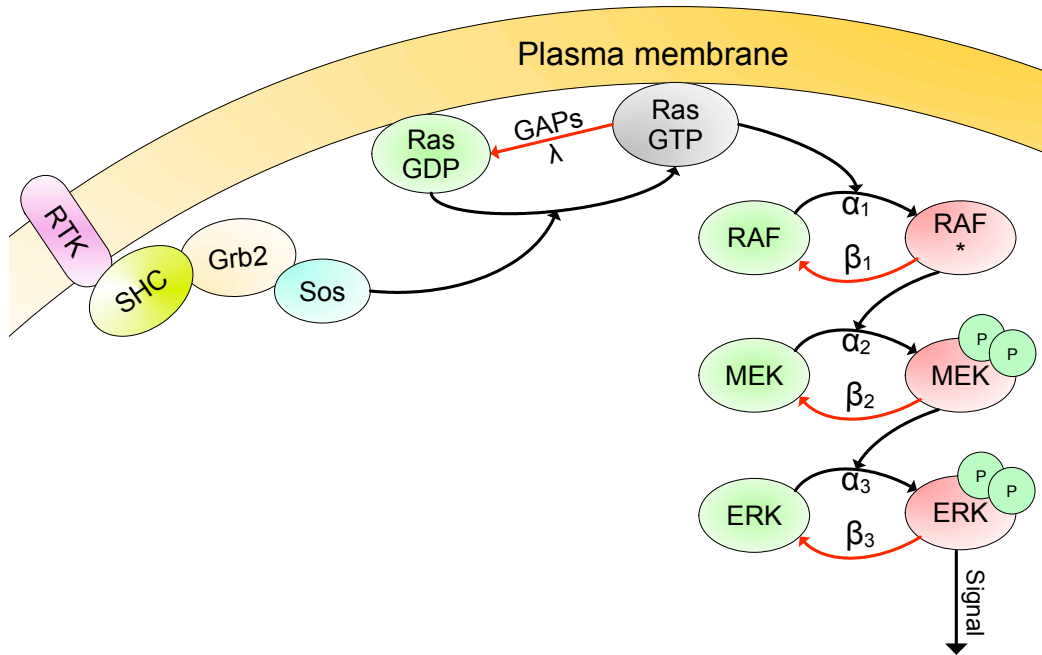


Figure 3.11: **Model of the Ras-ERK signaling pathway.** Mapping the parameters of the ordinary differential equation (Equation 3.1) by Heinrich et al. (2002) to the components of the Ras/RAF/MEK/ERK cascade. Symbols used: X_i denotes the concentration of active kinase i , α_i is the second-order rate constant for the phosphorylation of kinase i by kinase $(i - 1)$. β_i is a first-order rate constant for the dephosphorylation of kinase i and C_i is the total concentration of kinase i .

(for the first phosphorylation an increase of either 80 or 1000 fold activity, for a combined phosphorylation a 50000 fold increase). Since RAF is the central part in this cascade we next investigated how far known differences in activation and dephosphorylation could influence the output obtained from the cascade. Data indicate that B-RAF can be stronger activated whereas C-RAF is weaker activated.

The total concentrations of the respective kinases were set to values typical for eukaryotic cell lines reported by Ferrell (1996) ($C_{Ras} = 33$, $C_{RAF} = 17$, $C_{MEK} = 1300$, $C_{ERK} = 1250$). Values for α were estimated to be 600 for MEK and ERK. Based on kinetic data reported by Lew (2003) ($\alpha_{MEK} = 600$, $\alpha_{ERK} = 600$). Ras-GTP was assumed to have a half life of 10 minutes according to data from Qui and Green (1992) (setting of $\lambda = 0.069$; half life decay measured in seconds). Unfortunately, we could not apply experimentally proven β values for the respective phosphatases, however, we were able to

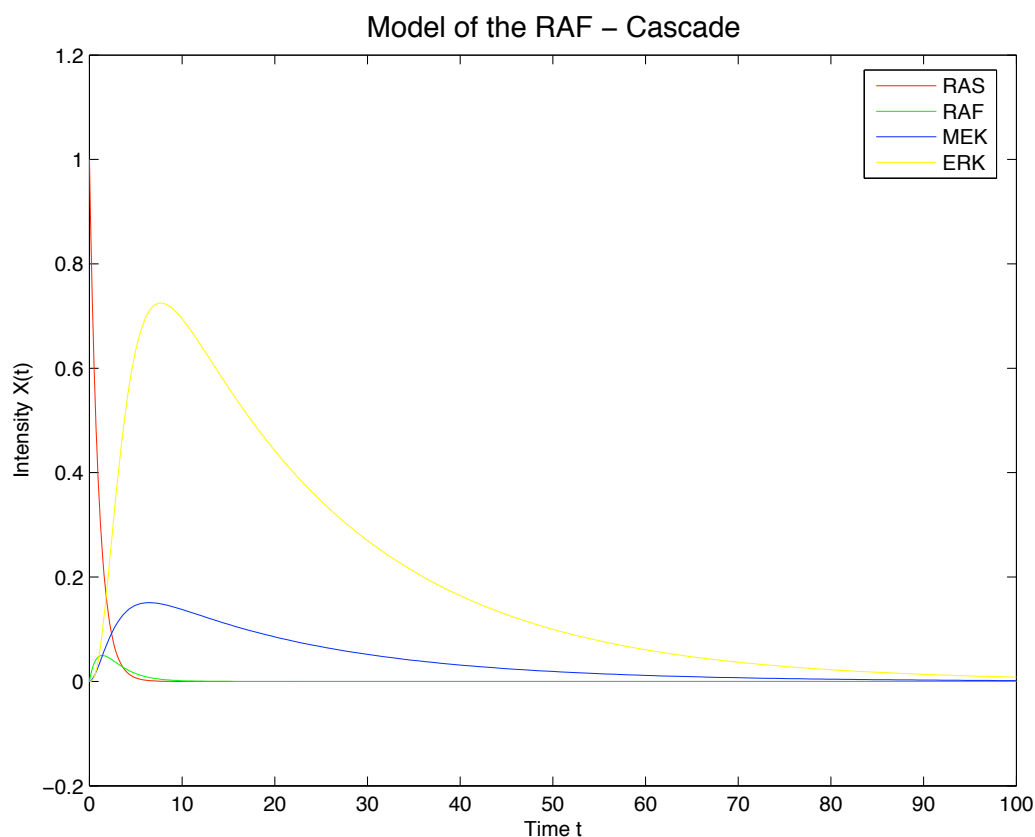


Figure 3.12: **Response curve for the Ras-ERK pathway under standard conditions.** An input signal activates the Ras receptor module with an exponential decay. Subsequent peaks of RAF, MEK and ERK follow each other with some time delay (time in arbitrary units) and the signal is amplified throughout the cascade. Parameters used for generating the graphs were: $\alpha_{RAF} = 0.1$, $\alpha_{MEK} = 1$, $\alpha_{ERK} = 5$, $\beta_{RAF} = 0.5$, $\beta_{MEK} = 0.5$, $\beta_{ERK} = 1$, $C_{Ras} = 1$, $C_{RAF} = 10$, $C_{MEK} = 20$, $C_{ERK} = 30$, $\lambda = 1$.

set sensible values for the phosphatases by applying kinetic parameters from the Brenda database (Schomburg et al., 2004). Since usually more than one phosphatase is involved in inactivation of the pathway, our estimations are only approximate ($\beta_{MEK} = 170$, $\beta_{ERK} = 170$). The situation is even more complex with RAF which is both positively and negatively regulated by phosphatases. Thus we could only estimate the β values taking into account the higher sensitivity for C-RAF kinase activity towards phosphatases. C-RAF requires phosphorylation on residues S338 and Y341 for complete activation. In B-RAF S445 (equivalent to S338 in C-RAF) is constitutively phosphorylated

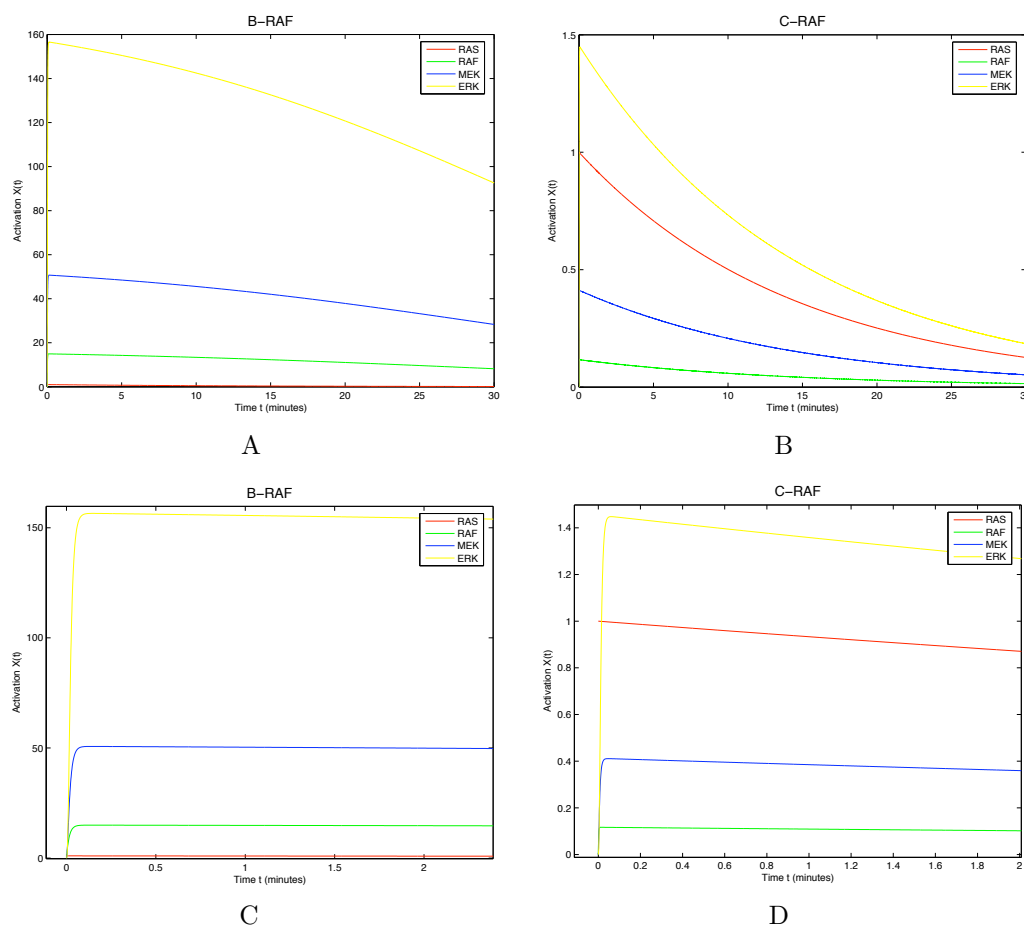


Figure 3.13: **Simulation showing the qualitative differences between B-RAF and C-RAF.** C-RAF shows a short-lived intense peak, decreasing quickly with time, whereas B-RAF shows a sustained strong activity. A rapid response of the cascade with almost no delay in the output signal mediated by ERK is observed for both RAF isoforms. We obtained different qualities for the signal peak mediated by B-RAF (**A** and **C**; same simulation but different scaling of the x-axis) compared to the peak mediated by C-RAF (**B** and **D**; same simulation but different scaling of the x-axis). The parameters used are shown in Table 3.2.

Parameter	Value	Reference
<i>Protein conc.</i>		
C_{Ras}	33	Ferrell (1996); Robubi et al. (2005)
C_{RAF}	17	Ferrell (1996); Robubi et al. (2005)
C_{MEK}	1300	Ferrell (1996); Robubi et al. (2005)
C_{ERK}	1250	Ferrell (1996); Robubi et al. (2005)
<i>Kinetic constants</i>		
λ	0.069	Qui and Green (1992); Robubi et al. (2005)
α_{RAF}	1000, 10	Robubi et al. (2005)
α_{MEK}	600	Lew (2003); Robubi et al. (2005)
α_{ERK}	600	Lew (2003); Robubi et al. (2005)
β_{RAF}	8, 80	Robubi et al. (2005)
β_{MEK}	170	Robubi et al. (2005)
β_{ERK}	170	Robubi et al. (2005)

Table 3.2: **Parameter values** for the simulations of the Ras/RAF/MEK/-ERK cascade (Figure 3.11). The simulation results are presented in Figure 3.13; based on the set of ordinary differential equations (Equation 3.1) by Heinrich et al. (2002).

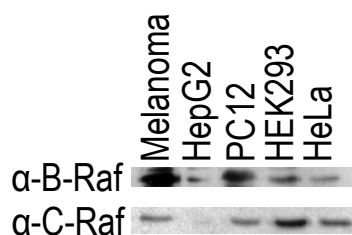


Figure 3.14: **Gel showing different expression levels of RAF kinases in different tissues.** The total kinase concentration can have profound effects on signal intensity, but only a slight effect on signal duration, which in our model depend primarily on the kinetic parameters. The protein concentrations for several cell types are shown. Equal amounts of total protein (25 μ g) were loaded.

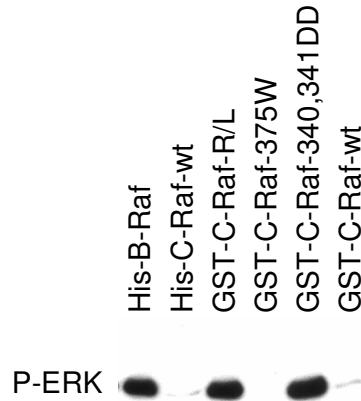


Figure 3.15: **Kinase assays showing the activity of different preparations of RAF kinases** purified from Sf9 cells. The protein purification, the assay conditions, and the immuno blotting are described in Materials and Methods. B-RAF shows far higher kinase activity than C-RAF, irrespective of the tag. However, C-RAF-Y340D/Y341D shows high kinase activity, as does C-RAF-R/L, for which C-RAF was coexpressed with oncogenic RasV12 and Lck. C-RAF-K375W shows no kinase activity (negative control). The range between 25 and 50 kDa is shown. P-ERK has a mass of approximately 42 kDa. No further bands were detected.

and the Y341 residue is replaced by aspartate. Thus B-RAF is primed for activation and more resistant against inactivation (Garnett and Marais, 2004).

Furthermore, we tested a range of parameter values, additional data and plots are shown in Figure A.1 in Appendix A (the wide range of parameters investigated leads to different scales on the y-axis of the plots). The plots in Figure 3.13 are close to the real situation: using the above available data and estimates and combining them with our model formalism, we obtained different qualities for the signal peak mediated by B-RAF compared to the peak mediated by C-RAF (Figure 3.13). The specific parameters estimated for B-RAF ($\alpha_{B-RAF} = 1000$, $\beta_{B-RAF} = 8$) lead to a broad, concave peak (Figure 3.13A) and with an almost constant behavior for the output signal in the early time steps (Figure 3.13C). Note furthermore, that parameters we estimate to be present in the tissue change the behavior of the cascade from that in Figure 3.12 into a rapid response of the cascade with almost no delay in the output signal mediated by ERK (Figure 3.13C, within seconds the cascade is also at top activation for ERK). This rapid signal mediation is also observed for C-RAF (Figure 3.13D; $\alpha_{C-RAF}=10$, $\beta_{C-RAF}=80$). However, the response curve is qualitatively different, of convex shape and leads to

an intensive short peak which is rapidly declining. Of course it is only a simplified model, however, we took for most parameters available biochemical data which allow us to demonstrate that indeed B-RAF behaves qualitatively differently from C-RAF.

The tissue-specific graphs in Figure 3.13 model the qualitative differences which exists between B-RAF (sustained, high level on state) and C-RAF (short high peak, then going down quickly with time): in the cellular cascade the phosphatases react fast leading to quick inactivation. C-RAF is quickly active (steep and strong signal amplitude), but also quickly deactivated. B-RAF is somewhat slower active, but very slowly inactivated, its activity curve also in the model follows somewhat Ras-GTP.

Furthermore, if we now take Table 1.2 into account, we realize that the parameters for activated B-RAF are indeed well suited to mediate functions known for B-RAF, i.e. cell cycle arrest and differentiation, whereas the transient, intensive peak predicted for C-RAF should explain why for C-RAF often a proliferation response is observed. The overall signal in a cell which has both RAF isoformes would of course be a combination of both effects.

According to this model we would expect and predict that in various cell types the distribution of B-RAF and C-RAF is in fact different to allow mediation of different cellular responses in a variety of tissues. To further support this, we investigated the respective amount of B-RAF and C-RAF in various cell lines (Figure 3.14). The protein concentrations for several cell types are shown. Equal amounts (determined by direct colorimetric assay, see Materials and Methods) of total protein (25 μg) were loaded to allow comparisons between different cell lines. As the immuno blot data indicate, B-RAF is present in high amounts in melanoma cells, HepG2 cells and PC12 cells, whereas C-RAF is the more dominating RAF in HEK293 cells and HeLa cells. We can thus indeed demonstrate a strong variation of B-RAF and C-RAF in these different cell lines. Note that the levels of B-RAF as well as of C-RAF isoforms change in specific tissues. Our immuno blots provide a good estimate of the relative changes regarding one isoform in different tissues and show that levels for one isoform do vary in different tissues. In contrast, the exact ratio between B-RAF and C-RAF is only approximated by the band intensities as different antibodies were used for each isoform.

To test our model predictions in respect of kinase activity differences we expressed tagged RAF kinases in Sf9 cells and performed a coupled kinase assay on the purified proteins (Figure 3.15).

We can show that B-RAF performs a high kinase activity without any specific intervention whereas C-RAF kinase activity is comparatively low. Quantitatively the difference in activities is about two orders of magnitude. The model prediction for comparison is an 180 fold difference of RAF kinase

activity, resulting in a 100 fold difference for ERK kinase activity at the end of the cascade (Figure 3.13). To obtain highly active C-RAF the model prediction suggests that the effect of the phosphatase is a critical aspect. One way to explore this experimentally would be to treat cells with phosphatase inhibitors prior to stimulation and assay immunoprecipitates of RAF kinases for activity. However dephosphorylation is important also for RAF kinase activation and treatment of cells with unspecific phosphatase inhibitors, such as Okadaic acid, was in fact shown to block activation of C-RAF (Kubicek et al., 2002). The effect of the phosphatase can be tested more specifically by genetic experiments with mutations. The important phosphorylation sites for activation in C-RAF are Y340 and Y341 as has been shown by previous investigations (Mason et al., 1999). We mutated these to aspartate residues to mimic constant phosphorylation. In fact, the resulting mutations at the phosphorylation sites Y340/Y341 to aspartates (equivalent to D447/D448 in B-RAF) lead to a greatly increased kinase activity in C-RAF (Figure 3.15). In an additional test we show that Lck, a tyrosine kinase able to phosphorylate C-RAF at 340/341, achieves the same effect if it is coexpressed together with RasV12 (Figure 3.15, lane GST-C-RAF-R/L). Thus also the experimental data support that the two RAF isoforms differ mainly in their sensitivity towards phosphatases.

3.3 DiRas3

3.3.1 DiRas3 interacts *in vitro* efficiently with active C-RAF and MEK.

To test *in vitro* the *in vivo* binding data regarding C-RAF association with DiRas3 we used BIAcore technology. For that purpose, purified GST-tagged C-RAF or MEK were immobilized to a CM5 chip coated with anti-GST antibody. Next the association and dissociation with purified DiRas3 were monitored (Figure 3.16, Figure 3.17A). In accordance with our *in vivo* results DiRas3 bound with high affinity to C-RAF activated with RasV12 and Lck (C-RAF-R/L) compared to non-activated C-RAF. While the Ras binding domain (RBD) of C-RAF did not bind DiRas3, the catalytic domain of C-RAF (C-RAF-BXB-Y340D/Y341D, designated as C-RAF-CT-DD) exhibited high binding affinity. Surprisingly, the most efficient binding to DiRas3 was recorded with purified MEK. Thus, DiRas3 interacts *in vitro* with the catalytic domain of C-RAF and even better with MEK. The apparent affinity constants (K_D values) revealed that MEK binding was about four fold higher than binding of DiRas3 to active C-RAF (0.18 μ M and 0.80 μ M respectively). In

comparison the binding of DiRas3 to MEK was even 2.5 times stronger than the interaction between H-Ras-GTP and C-RAF (0.18 μM versus 0.46 μM).

3.3.2 Inhibition of MEK activity by DiRas3 *in vitro*.

To investigate the influence of His-DiRas3 and His- ΔN -DiRas3 on kinase activities of the RAF-MEK-ERK signalling cascade we performed coupled kinase assays using an active mutant of C-RAF, GST-C-RAF-Y340D/Y341D (designated as C-RAF-DD), purified MEK-1 and ERK-2 and increasing concentrations of His-DiRas3 or His- ΔN -DiRas3. Surprisingly, DiRas3 inhibited ERK phosphorylation by MEK but not MEK phosphorylation by C-RAF (Figure 3.17B). The N-terminally truncated DiRas3 inhibited MEK activity to a much lower degree (compare lane 4–6 with 7–9). But again no effect on C-RAF activity was detected.

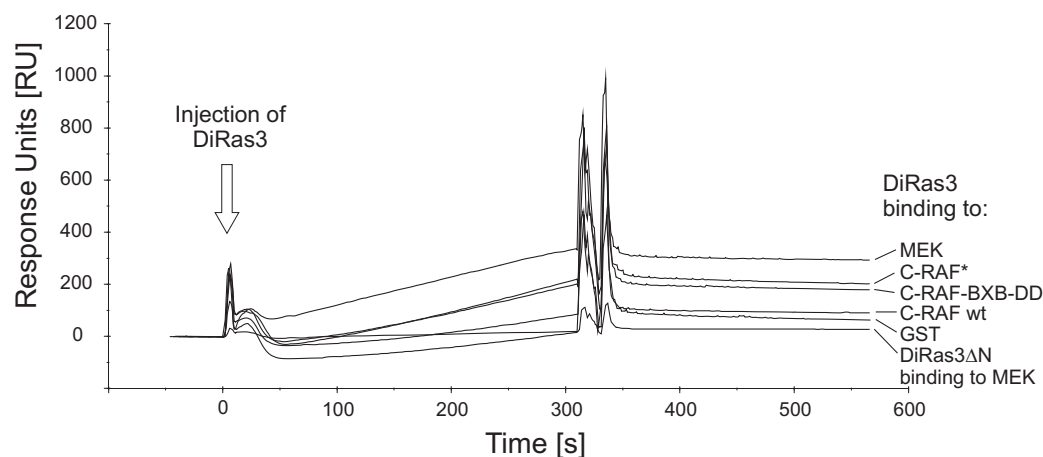


Figure 3.16: DiRas3 interaction with C-RAF and MEK—BIAcore. The biosensor chip CM5 was loaded with anti-GST antibody using covalent derivatization. GST-tagged proteins were immobilized on the biosensor which resulted in a deposition of approximately 800–1200 response units (RU). Next purified DiRas3-GDP was injected. The unspecific binding was measured in the reference cell and subtracted. DiRas3 binds efficiently to MEK and active C-RAF preparations (C-RAF*, C-RAF-BXB-DD), but reveals no significant binding to inactive C-RAF wild type (wt). The association rates differ between the probes, whereas the dissociation rate is similar and very low for all the probes tested. GST is used as a negative control. GST ΔN -DiRas3 shows no significant binding to MEK nor any other protein tested (data not shown).

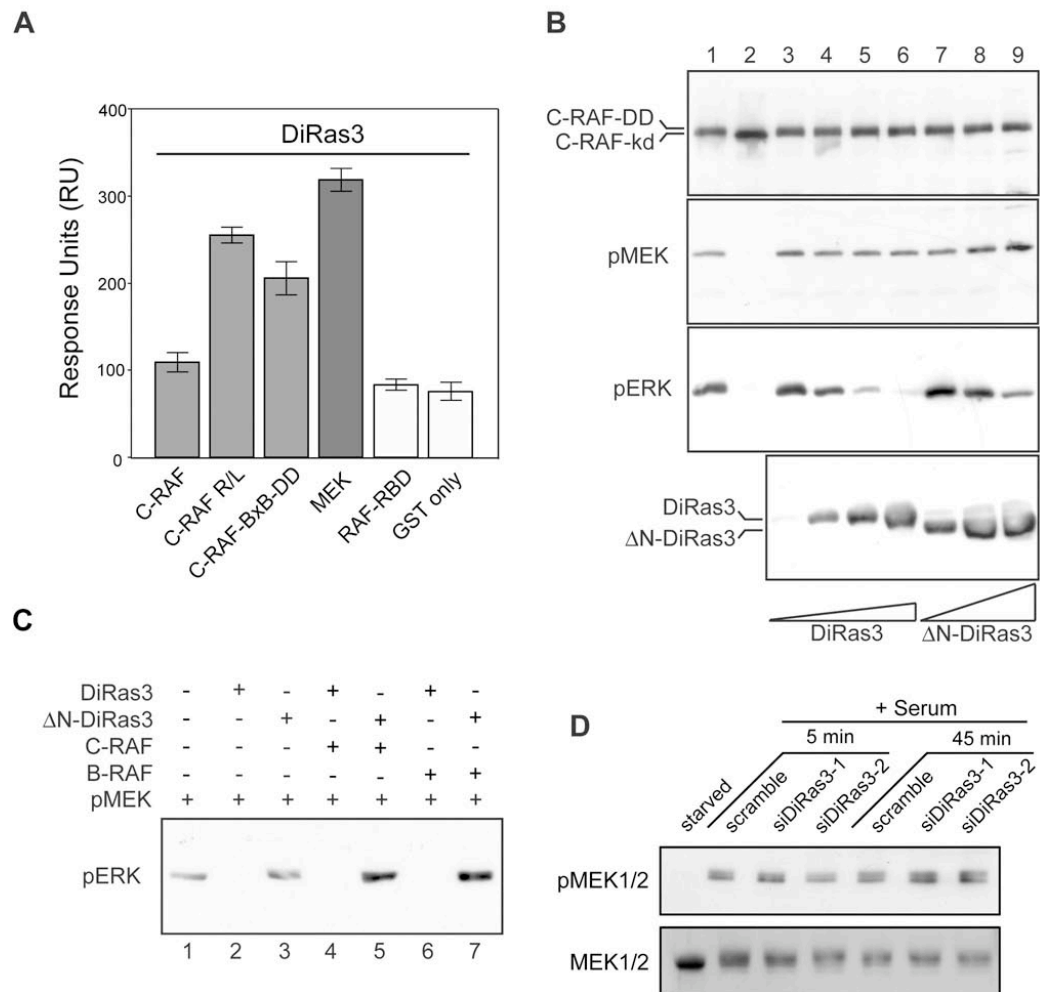


Figure 3.17: DiRas3 interaction with C-RAF and MEK. **A:** Biosensor analysis. A CM5 sensor chip was loaded with anti-GST antibody using covalent derivatization. Purified GST-tagged MEK, full-length C-RAF, C-RAF-RBD, and a constitutively active C-terminal part of C-RAF (C-RAF-BXB-DD) were immobilized considering their molecular size. Following DiRas3-GDP injection (400 nM) association-dissociation curves were monitored. The bar represents the maximal association degrees. **B–C)** DiRas3 inhibits MEK but not C-RAF in *in vitro* kinase assays. **B:** The effect of DiRas3 on MEK and ERK phosphorylation were monitored by use of an *in vitro* kinase assay with equal concentrations of purified MEK-1, ERK-2 and GST-C-RAF-Y340D/Y341D (C-RAF-DD). The assay conditions were as described in Materials and Methods. Lane1: no DiRas3; lane2: kinase dead GST-C-RAF-K375W was used as a negative control; lanes 3–6: 0.1 μ g, 0.5 μ g, 1 μ g, and 1.5 μ g DiRas3-GDP; lanes 7–9: 1 μ g, 3 μ g, 5 μ g Δ N-DiRas3-GDP. **C:** ERK-2 was phosphorylated by active MEK-1 in presence of DiRas3 (1.5 μ g) or Δ N-DiRas3 (1.5 μ g) alone, in presence of GST-C-RAF-DD (0.5 μ g) or His-B-RAF (0.5 μ g). **D:** This experiment was performed by Beck et al. MCF10A cells treated with si-oligos targeting DiRas3 were starved, stimulated with serum, after indicated time points lysed and analysed by immunoblot detecting total MEK and pMEK levels.

To investigate whether the inhibition of MEK by DiRas3 is C-RAF dependent, a MEK-ERK assay was performed omitting C-RAF. Active MEK was obtained by *in vitro* phosphorylation of purified MEK-1 using B-RAF and subsequent removal of B-RAF as described in Materials and Methods. The MEK preparation obtained was highly active but not quantitatively phosphorylated. DiRas3 inhibited the kinase activity of MEK irrespective of the addition of active C-RAF or B-RAF (Figure 3.17C). On the other hand, no suppression of kinase activity was detected in the presence of Δ N-DiRas3. In fact, in the presence of active RAF kinases, ERK phosphorylation was elevated compared to the MEK probe (lane 1), presumably because the MEK preparation was not completely phosphorylated and the presence of active RAF kinases led to elevation of pERK. Based on these results we conclude that DiRas3 is a specific MEK inhibitor and that RAF kinases are not required for this effect.

Consequently Beck et al. studied the effect of DiRas3 on MEK phosphorylation *in vivo*. In DiRas3 downregulated MCF10A cells no difference in MEK phosphorylation compared to control cells was detectable (Figure 3.17D). However, as ERK phosphorylation was modified in comparable experiments (Beck et al.–submitted), we conclude that DiRas3 did not inhibit or alter MEK phosphorylation but reduced MEK activity to phosphorylate ERK. Thus, we provide here *in vitro* and *in vivo* evidence that DiRas3 is a MEK inhibitor.

Chapter 4

Discussion

4.1 Developing a novel RAF kinase inhibitor

In search for a novel irreversible RAF kinase inhibitor, we were stimulated by the unique cysteine 532 residue (B-RAF numbering, GI:50403720). The high reactivity of the epoxide moiety was a challenging task for the synthesis. The approach to provide oxiranylcarboxylic acid (**5**) described in the literature (Grosjean et al., 1994) did not work in our hands. Eventually a novel synthetic approach including a lyophilization step let ultimately to **5**. We started the synthesis with racemic serine and therefore obtained **4** as a racemate. However, our synthetic strategy is well suited for the synthesis of enantiopure **4** and therefore also compound **1**.

Compound **1** showed a clear and direct RAF kinase inhibition *in vitro*, albeit weaker than BAY 43-9006 (Figure 3.4 and Table 3.1), indicating that it is delivered to the targeted site in the kinase domain. However, kinetic and mass spectroscopic experiments strongly argue that the inhibitor was probably not covalently bound to the specific cysteine residue. The homology

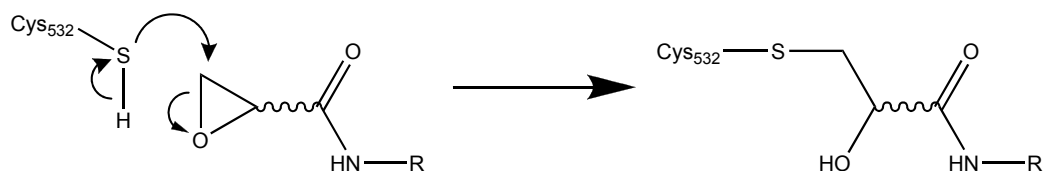


Figure 4.1: **Reaction mechanism between a cysteine and an epoxide.** The nucleophilic sulfur atom of the cysteine can only attack and covalently bind to the epoxide moiety if the back of the beta carbon atom is exposed to it. See also Figure 3.2 on page 41 and Appendix A for a three dimensional view.

model and the *in vitro* data indicate that compound **1** can successfully bind to the targeted site, however the orientation of the epoxide moiety relative to the nucleophilic sulfur atom is crucial: the sulfur atom needs to attack the epoxide group from the back of the beta carbon (Figure 4.1). The natural ligand at this site is the planar purine ring system of ATP. The epoxide moiety is probably ill suited to mimic this electron-rich π -ring system. The corresponding acrylamide derivative did also not show an irreversible inhibition of RAF kinases in our time kinetics analysis (data not shown).

Compound **1** did not inhibit RAF kinases in cell culture. In fact, in RAF transformed cell lines, the compound even strongly activated the mitogenic signaling pathway. RAF activation through ZM 336372 or SB 203580 was usually explained by feedback regulation of RAF (Figure 4.2A). Inhibition of RAF also leads to inhibition of negative feedback regulation and therefore to activation (in the absence of the inhibitor). Negative feedback regulation is described at the level of SOS (Chen et al., 1996) as well as RAF (Brummer et al., 2003; Dougherty et al., 2005; Hekman et al., 2005). However, the fact that inhibitors of MEK do not cause this activation argues against that hypothesis. It appears more likely that a different target X is affected by RAF inhibitors (Figure 4.2B). This different target may be RAF itself if the activation *in vivo* relies on oligomerization of RAF kinases (Rushworth et al., 2006). Such an oligomerization has already been hypothesized for SB 203580 but was not experimentally shown (Hall-Jackson et al., 1999b). Although no evidence for oligomerization was obtained *in vitro*, experiments with RAF knockout cells were consistent with this hypothesis. An alternative explanation might be the inhibition of an inhibitory kinase. All protein kinases with Thr106 (p38 α numbering) could be candidates for such a role (Hall-Jackson et al., 1999b)(see Appendix A). However, this criterion is not that strict for diphenyl urea compounds as some non-Thr106 kinases (such as VEGFRs) are also potentially targeted by such inhibitors.

Compound **1** is the first diphenyl urea compound for which an activation of RAF kinases in cell culture was described. The implications this may have for BAY 43-9006 and other compounds are not clear. BAY 43-9006 is a rather non specific inhibitor with activity against a wide range of important targets. It blocks the mitogenic signaling pathway in many tumor cell lines, but not in human non-small-cell lung cancer (NSCLC) carcinoma lines. This may be due to a RAF independent activation of MEK in this cell line (Wilhelm et al., 2004). However, BAY 43-9006 also failed to impair ERK phosphorylation and reduce tumor size in a transgenic mouse tumor model with C-RAF driven lung adenomas, arguing against a RAF independent mechanism of MEK activation in lung cancer. In the same mouse model, treatment with CI-1040 (PD 184352), a potent MEK inhibitor, lead to a significant reduction

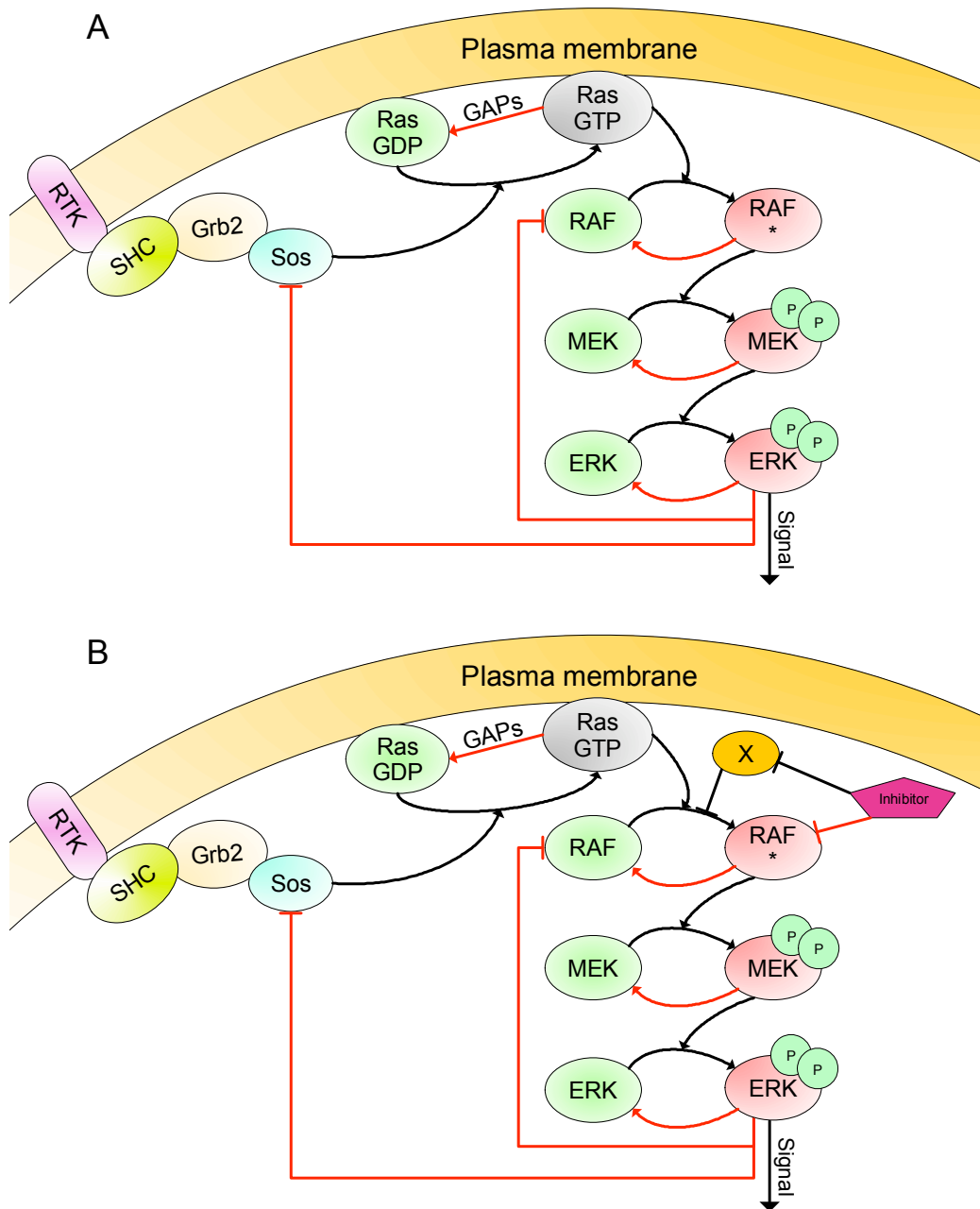


Figure 4.2: **Model of the mitogenic signaling pathway.** **A:** Negative feedback regulation has been reported at the level of SOS (Chen et al., 1996) and RAF (Brummer et al., 2003; Dougherty et al., 2005; Hekman et al., 2005). **B:** RAF kinase inhibitors may however activate by binding to a protein X which may facilitate its activation. This protein might in fact be RAF itself (Hall-Jackson et al., 1999b). However we were not able to detect increased RAF association upon treatment with inhibitor. The differences observed in different cell type (Hall-Jackson et al., 1999b; Wilhelm et al., 2004) also suggest that protein X is a different protein kinase.

of ERK phosphorylation and adenoma size (Kramer et al., 2004). Therefore a conditional RAF activation by BAY 43-9006 can at least not be ruled out.

We have set up the entire route for the development of a kinase inhibitor targeted against an Thr106 and Cys109 (p38 α numbering) protein kinase RAF including molecular modeling, the synthesis, *in vitro* assay, cell culture, and mass spectrometry. Given that there are only 14 genes in the human genome coding for with a Thr106 and Cys109 kinase domain (Speg, PDGFR α , PDGFR β , Kit, Fms, KSR, ANP-A, ANP-B, RETGC-1, RETGC-2, NEK11, and A-, B-, and C-RAF), a specific irreversible RAF kinase inhibitor on this basis is a real perspective and—in the opinion of the author—needs to be pursued further.

4.2 Dynamic modeling

We show here how tissue specific variation in RAF-response can be explained in terms of different distribution of B-RAF and C-RAF and their different response to activation by kinases and inactivation by phosphatases. In particular we could adopt a standard model of response by introducing more accurate parameters known from experimental data and show that this leads to qualitatively different behavior in B-RAF and C-RAF signaling. The differences in peak shape and length accord with their different effects on cells. To further support our hypothesis of differential effects in tissues by differential behavior of B-RAF and C-RAF we experimentally confirm that their quantitative distribution varies strongly in different cell lines. Certainly our analysis is based on a simplistic model but nevertheless it demonstrates that core signaling molecules existing in different isoforms can in fact mediate different tissue specific signals (Table 1.2, p. 30) for the concrete system of the RAF-MEK-ERK cascade.

Our mathematical model, which was based on a formalism for a linear signaling cascade described by Heinrich et al. (2002), but now takes different isoforms and their ratios into account, strongly simplifies a number of further factors that have been described in literature. In this study we did not take into account possible crosstalk with other signaling modules like Rap1 nor did we include negative feedback regulation (Dougherty et al., 2005; Hekman et al., 2005). A-RAF was not considered since it possesses the lowest kinase activity of the RAF kinases and is mostly expressed in urogenital tissue (Storm et al., 1990). We further simplified the complex regulation of RAF kinases by using single rate constants to calculate their activation and inactivation in our model.

More complex models include different terms producing more complex

results. Thus negative feedback regulation is an important factor in MAPK cascades. For example, this was predicted to lead to quantitative differences in the EGF and NGF signaling in PC12 cells. In this model which uses only one type of RAF this factor was found to be an important ingredient in determining cascade activation (Brightman and Fell, 2000). However, Yamada et al. (2004) did not find this effect in their simulations including feedback regulation. In contrast, they investigated the effect and found a significant role for fibroblast growth factor receptor substrate 2 (FRS2) in the NGF/FGF pathway regarding sustained MAPK activation. In this case the authors used a detailed model of the receptor activation including Grb2-SOS and FRS2. Thus differential effects of feedback regulation do have an important modulatory effect on the mitotic signaling pathway and duration of activation. Moreover, the feedback regulation of C-RAF (Dougherty et al., 2005) might be rather different from the partly ERK-mediated feedback in B-RAF (Brummer et al., 2003), however there is no quantitative data on B-RAF feedback regulation. Furthermore, these are in addition and separate from the effect of the different RAF isoforms, the focus of this study and modeled here in the simplified cascade shown in Figure 3.11 on page 52 based on parameters shown in Table 3.2 on page 55.

A clear limitation arises from our Ras term. It assumes that Ras-GTP is present at high concentrations at time point 0 and declines in a first order reaction. This is an approximation that doesn't hold true for most real systems. Note also that our model results are in line with a detailed model of Ras/RAF/MEK/ERK activation presented in a recent article by Sasagawa et al. (2005) focusing on the interplay between Ras and Rap1. For this model PC12 cells was considered and clearly distinct dynamics of transient and sustained ERK activation resulted by the rapid increase of epidermal growth factor and nerve growth factor but not on their final concentration. This was validated by measurements of ERK phosphorylation. Peyker et al. (2005) experimentally observed clear effector differences between different Ras isoforms. In the context of our model, different receptor tyrosine kinases possess different rates of deactivation. Slower rates of deactivation for receptor tyrosine kinases (and Ras) will lead to prolonged signals as seen in many cancer cells, whereas high expression levels cause higher signal intensities. The huge number of receptor tyrosine kinases suggests a high degree of regulation already at this step (Offterdinger et al., 2004). For simplicity, we did not consider complex effects of scaffolds and other factors further modifying and changing kinase activity in B-RAF and C-RAF. These complicating factors will be included in later studies. However, our model, despite of its simplicity, suggests different cellular responses (Table 1.2, p. 30) mediated by the different isoforms.

Before time series experiments provide detailed kinetic data on the complete cascade we can only conclude that our model is supported by all the kinetic data reported on the cascade so far and by the experimental data shown here on isoform specific different expression levels in different tissues and differential behavior of the RAF kinase isoforms against phosphatases.

The regulation of RAF kinases and B-RAF in particular is also a focus for cancer research. Mutations of B-RAF are detected in a number of tumors. Most mutations generate a B-RAF with elevated and constitutive kinase activity, however some B-RAF mutants possess impaired but nevertheless constitutive kinase activity. These rare mutations may coincide with Ras mutations which are not detected in tumors with highly activating B-RAF mutations. These data indicate that tumours depend on a prolonged but tightly modulated B-RAF signaling (Garnett and Marais, 2004).

Another point is that the concentration of RAF kinases might be rather dynamical for a given cell type (Cleveland et al., 1994). Higher protein expression levels of the kinases will elevate signal intensity but have almost no effect on signal duration which is primarily determined by kinetic properties and the expression levels of the phosphatases.

It might be assumed from comparison of both RAF kinases that C-RAF is not predominant. However, in situations for which activation by B-RAF alone is not sufficient, the additional activation by C-RAF may become critical. This depends on the quantitative ratio between B-RAF and C-RAF which was not yet accurately modeled here considering further modifying factors and scaffolds. Indeed, Trakul et al. (2005) showed in siRNA depletion experiments both C-RAF and B-RAF are important as the total RAF activity is reduced by 60% versus 90%, respectively, if one or the other RAF isoform is inactivated. In fact both are required as predicted, but further technical improvements will be necessary to get exact quantitative data. B- and C-RAF are almost equally important for the initial signal intensity but it is mostly B-RAF which is responsible for signal duration.

4.3 DiRas3

Results presented in this contribution demonstrate that DiRas3, a Ras-like GTPase, interacts with activated C-RAF and is a direct negative regulator of MEK activity. The interaction of DiRas3 with C-RAF is in several ways unusual. First, DiRas3 bound directly to the catalytic half of C-RAF (Figure 3.16, p. 59). It represents the first GTPase with such an affinity. Yet, we did not detect an inhibition of C-RAF kinase activity in an *in vitro* kinase assay where already activated C-RAF was used (Figure 3.17B, p. 60). Also

DiRas3 downregulation did not affect MEK phosphorylation (Figure 3.17D, Beck et al.–submitted). Though we did not detect a functional consequence of this interaction the function of other proteins binding to RAF like 14-3-3, paxillin, or KSR might be modified (McKay and Morrison, 2007). Second, DiRas3 and Ras-GTP can bind simultaneously to C-RAF. Additionally, DiRas3 increases the amount of Ras-GTP bound to the DiRas3-C-RAF-complex (Beck et al.–submitted).

This cooperativity might be caused by a DiRas3 mediated stabilization of a particular RAF conformation, which engages the CRD. Therefore, by blocking the RAF-kinase cascade, DiRas3 may trap Ras-GTP in signalling dead end RAF-complexes. C-RAF seems to act similarly to WASP (Wiskott-Aldrich syndrome protein) as an “and” gate, whereby integrating two distinct GTPase signals (Prehoda et al., 2000). The first signal, leading to the activation of Ras and the second one, leading to the association of DiRas3 to RAF seem to be both necessary for MEK inhibition at the plasma membrane. The second signal is likely to be triggered by steroid hormones, as DiRas3 is mainly expressed in ovarian and breast tissue (Yu et al., 1999), which undergo monthly cycles of proliferation and apoptosis. This scenario is supported by up to four different principles of expression regulation of DiRas3 (Yu et al., 2005). It remains to be established whether DiRas3 interacts also with A-

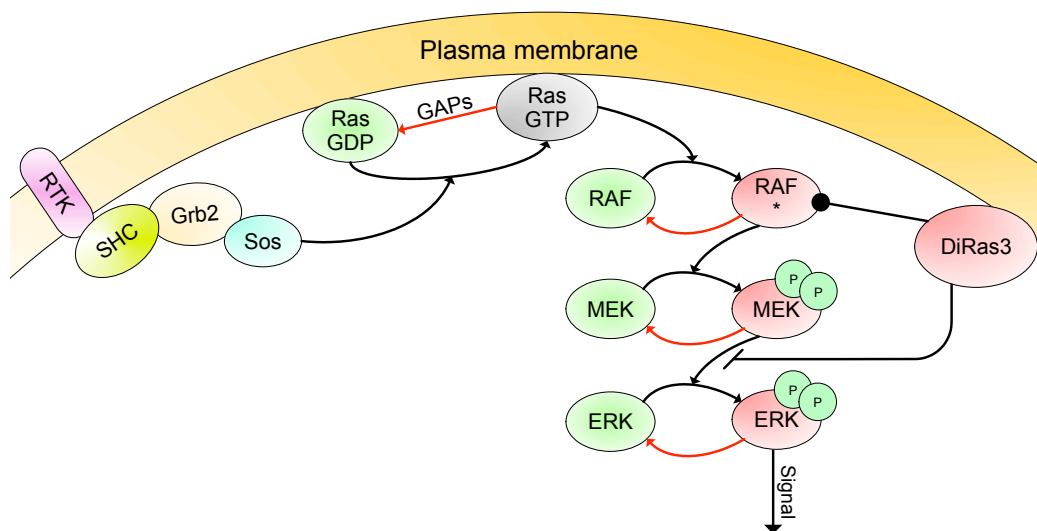


Figure 4.3: **DiRas3 binds to RAF as well as to MEK and blocks MEK from phosphorylating ERK.** A detailed description of the signaling cascade is given in Figure 1.2 on page 24. Our data show clearly that DiRas3 does not inhibit RAF kinases despite binding to C-RAF.

and B-RAF.

Based on our data, we propose the following model for the regulation of the mitogenic signalling cascade by DiRas3: signal induced Ras-GTP recruits C-RAF within the plasma membrane to initiate RAF activation. Thereafter DiRas3 can bind to the open conformation of C-RAF. Beck et al. identified AA150–331 of C-RAF encompassing the CRD and CR2, and the catalytic CR3 domain in C-RAF, as potential binding interfaces between DiRas3 and C-RAF (Beck et al.–submitted). Not all of these domains may be bound simultaneously to DiRas3. Remarkably, 14-3-3 proteins bind to CR2 and CR3 and upregulate RAF kinase activity as shown in several model organisms (Wilker and Yaffe, 2004). Thus, DiRas3 may displace *in vivo* 14-3-3 from RAF to downregulate the RAF activity. Consistently, DiRas3 did not interfere with RAF activity in the *in vitro* assays, where already activated RAF kinase was used. The binding of DiRas3 to the CR3 region of C-RAF may also result in reduced access of activating kinases or in impaired binding of the substrates of the RAF kinase. Thus, DiRas3 might negatively influence the complete RAF activation within the plasma membrane. In addition to its ability to bind active C-RAF in the plasma membrane, we demonstrate here that DiRas3 can efficiently associate with MEK and inhibit its kinase activity. Interestingly, *in vitro* and *in vivo* experiments demonstrate that phosphorylation of MEK by C-RAF is not influenced by DiRas3. The signal transduction from MEK to ERK is however nearly abolished in the presence of DiRas3 (Figure 3.17, p. 60). Thus, DiRas3 might not only influence the activation of C-RAF but it might also need active C-RAF to inhibit MEK suggesting a scaffold function (Figure 4.3).

Efficient activation of RAF needs the redistribution of Ras-GTP from raft micro domains into non-raft regions of the plasma membrane (Prior et al., 2001). Therefore, a similar relocation of the RAF-DiRas3-complex at the plasma membrane, may release the binding domain of DiRas3 that is needed for MEK association. We suggest that a change of lipid micro-environment may induce association of DiRas3 with MEK terminating RAF signaling.

Bibliography

L. F. Allen, P. F. Lenehan, I. A. Eiseman, W. L. Elliott, and D. W. Fry. Potential benefits of the irreversible pan-erbB inhibitor, CI-1033, in the treatment of breast cancer. *Semin Oncol*, 29(3 Suppl 11):11–21, Jun 2002. 41

Y. Aoki, T. Niihori, H. Kawame, K. Kurosawa, H. Ohashi, Y. Tanaka, M. Filocamo, K. Kato, Y. Suzuki, S. Kure, and Y. Matsubara. Germline mutations in HRAS proto-oncogene cause Costello syndrome. *Nat Genet*, 37(10):1038–1040, Oct 2005. doi: 10.1038/ng1641. URL <http://dx.doi.org/10.1038/ng1641>. 22

T. I. Bonner, S. B. Kerby, P. Sutrave, M. A. Gunnell, G. Mark, and U. R. Rapp. Structure and biological activity of human homologs of the raf/mil oncogene. *Mol Cell Biol*, 5(6):1400–1407, Jun 1985. URL <http://www.pubmedcentral.nih.gov/articlerender.fcgi?tool=pubmed&pubmedid=2993863>. 20

F. A. Brightman and D. A. Fell. Differential feedback regulation of the MAPK cascade underlies the quantitative differences in EGF and NGF signalling in PC12 cells. *FEBS Lett*, 482(3):169–174, Oct 2000. doi: 10.1016/S0014-5793(00)02037-8. URL [http://dx.doi.org/10.1016/S0014-5793\(00\)02037-8](http://dx.doi.org/10.1016/S0014-5793(00)02037-8). 67

T. Brummer, H. Naegele, M. Reth, and Y. Misawa. Identification of novel ERK-mediated feedback phosphorylation sites at the C-terminus of B-Raf. *Oncogene*, 22(55):8823–8834, Dec 2003. doi: 10.1038/sj.onc.1207185. URL <http://dx.doi.org/10.1038/sj.onc.1207185>. 24, 64, 65, 67

L.-F. Bélanger, S. Roy, M. Tremblay, B. Brott, A.-M. Steff, W. Mourad, P. Hugo, R. Erikson, and J. Charron. Mek2 is dispensable for mouse growth and development. *Mol Cell Biol*, 23(14):4778–4787, Jul 2003. doi: 10.1128/MCB.23.14.4778-4787.2003. URL <http://dx.doi.org/10.1128/MCB.23.14.4778-4787.2003>. 23

- S. L. Campbell, R. Khosravi-Far, K. L. Rossman, G. J. Clark, and C. J. Der. Increasing complexity of Ras signaling. *Oncogene*, 17(11 Reviews): 1395–1413, Sep 1998. doi: 10.1038/sj.onc.1202174. URL <http://dx.doi.org/10.1038/sj.onc.1202174>. 24
- B. J. Canagarajah, A. Khokhlatchev, M. H. Cobb, and E. J. Goldsmith. Activation mechanism of the MAP kinase ERK2 by dual phosphorylation. *Cell*, 90(5):859–869, Sep 1997. doi: 10.1016/S0092-8674(00)80351-7. URL [http://dx.doi.org/10.1016/S0092-8674\(00\)80351-7](http://dx.doi.org/10.1016/S0092-8674(00)80351-7). 23
- F. Carlomagno, S. Anaganti, T. Guida, G. Salvatore, G. Troncone, S. M. Wilhelm, and M. Santoro. BAY 43-9006 inhibition of oncogenic RET mutants. *J Natl Cancer Inst*, 98(5):326–334, Mar 2006. doi: 10.1093/jnci/djj069. URL <http://dx.doi.org/10.1093/jnci/djj069>. 21
- P. Chardin. GTPase regulation: getting aRnd Rock and Rho inhibition. *Curr Biol*, 13(18):R702–R704, Sep 2003. doi: 10.1016/j.cub.2003.08.042. URL <http://dx.doi.org/10.1016/j.cub.2003.08.042>. 31
- D. Chen, S. B. Waters, K. H. Holt, and J. E. Pessin. SOS phosphorylation and disassociation of the Grb2-SOS complex by the ERK and JNK signaling pathways. *J Biol Chem*, 271(11):6328–6332, Mar 1996. doi: 10.1074/jbc.271.11.6328. URL <http://dx.doi.org/10.1074/jbc.271.11.6328>. 24, 64, 65
- P. C. Chin, L. Liu, B. E. Morrison, A. Siddiq, R. R. Ratan, T. Bottiglieri, and S. R. D’Mello. The c-Raf inhibitor GW5074 provides neuroprotection in vitro and in an animal model of neurodegeneration through a MEK-ERK and Akt-independent mechanism. *J Neurochem*, 90(3):595–608, Aug 2004. doi: 10.1111/j.1471-4159.2004.02530.x. URL <http://dx.doi.org/10.1111/j.1471-4159.2004.02530.x>. 28, 45
- J. L. Cleveland, J. Troppmair, G. Packham, D. S. Askew, P. Lloyd, M. González-García, G. Nuñez, J. N. Ihle, and U. R. Rapp. v-raf suppresses apoptosis and promotes growth of interleukin-3-dependent myeloid cells. *Oncogene*, 9(8):2217–2226, Aug 1994. 68
- H. Davies, G. R. Bignell, C. Cox, P. Stephens, S. Edkins, S. Clegg, J. Teague, H. Woffendin, M. J. Garnett, W. Bottomley, N. Davis, E. Dicks, R. Ewing, Y. Floyd, K. Gray, S. Hall, R. Hawes, J. Hughes, V. Kosmidou, A. Menzies, C. Mould, A. Parker, C. Stevens, S. Watt, S. Hooper, R. Wilson, H. Jayatilake, B. A. Gusterson, C. Cooper, J. Shipley, D. Hargrave, K. Pritchard-Jones, N. Maitland, G. Chenevix-Trench, G. J. Riggins, D. D. Bigner, G. Palmieri, A. Cossu, A. Flanagan, A. Nicholson, J. W. C. Ho, S. Y. Leung, S. T. Yuen,

- B. L. Weber, H. F. Seigler, T. L. Darrow, H. Paterson, R. Marais, C. J. Marshall, R. Wooster, M. R. Stratton, and P. A. Futreal. Mutations of the BRAF gene in human cancer. *Nature*, 417(6892):949–954, Jun 2002. doi: 10.1038/nature00766. URL <http://dx.doi.org/10.1038/nature00766>. 19, 20, 21, 23
- P. Dent, W. Haser, T. A. Haystead, L. A. Vincent, T. M. Roberts, and T. W. Sturgill. Activation of mitogen-activated protein kinase kinase by v-Raf in NIH 3T3 cells and in vitro. *Science*, 257(5075):1404–1407, Sep 1992. doi: 10.1126/science.1326789. URL <http://dx.doi.org/10.1126/science.1326789>. 22
- M. K. Dougherty, J. Müller, D. A. Ritt, M. Zhou, X. Z. Zhou, T. D. Copeland, T. P. Conrads, T. D. Veenstra, K. P. Lu, and D. K. Morrison. Regulation of Raf-1 by direct feedback phosphorylation. *Mol Cell*, 17(2):215–224, Jan 2005. doi: 10.1016/j.molcel.2004.11.055. URL <http://dx.doi.org/10.1016/j.molcel.2004.11.055>. 24, 64, 65, 66, 67
- N. Duesbery and G. V. Woude. BRAF and MEK mutations make a late entrance. *Sci STKE*, 2006(328):pe15, Mar 2006. doi: 10.1126/stke.3282006pe15. URL <http://dx.doi.org/10.1126/stke.3282006pe15>. 20, 21
- M. A. Farrar, Alberol-Ila, and R. M. Perlmutter. Activation of the Raf-1 kinase cascade by coumermycin-induced dimerization. *Nature*, 383(6596):178–181, Sep 1996. doi: 10.1038/383178a0. URL <http://dx.doi.org/10.1038/383178a0>. 45
- W. Feng, Z. Lu, R. Z. Luo, X. Zhang, E. Seto, W. S.-L. Liao, and Y. Yu. Multiple histone deacetylases repress tumor suppressor gene ARHI in breast cancer. *Int J Cancer*, 120(8):1664–1668, Apr 2007. doi: 10.1002/ijc.22474. URL <http://dx.doi.org/10.1002/ijc.22474>. 31
- J. E. Ferrell. Tripping the switch fantastic: how a protein kinase cascade can convert graded inputs into switch-like outputs. *Trends Biochem Sci*, 21(12):460–466, Dec 1996. doi: 10.1016/S0968-0004(96)20026-X. URL [http://dx.doi.org/10.1016/S0968-0004\(96\)20026-X](http://dx.doi.org/10.1016/S0968-0004(96)20026-X). 38, 52, 55
- D. W. Fry. Mechanism of action of erbB tyrosine kinase inhibitors. *Exp Cell Res*, 284(1):131–139, Mar 2003. doi: 10.1016/S0014-4827(02)00095-2. URL [http://dx.doi.org/10.1016/S0014-4827\(02\)00095-2](http://dx.doi.org/10.1016/S0014-4827(02)00095-2). 41
- M. J. Garnett and R. Marais. Guilty as charged: B-RAF is a human oncogene. *Cancer Cell*, 6(4):313–319, Oct 2004. doi: 10.1016/j.ccr.2004.09.022. URL <http://dx.doi.org/10.1016/j.ccr.2004.09.022>. 25, 56, 68

S. Giroux, M. Tremblay, D. Bernard, J. F. Cardin-Girard, S. Aubry, L. Larouche, S. Rousseau, J. Huot, J. Landry, L. Jeannotte, and J. Charon. Embryonic death of Mek1-deficient mice reveals a role for this kinase in angiogenesis in the labyrinthine region of the placenta. *Curr Biol*, 9(7):369–372, Apr 1999. doi: 10.1016/S0960-9822(99)80164-X. URL [http://dx.doi.org/10.1016/S0960-9822\(99\)80164-X](http://dx.doi.org/10.1016/S0960-9822(99)80164-X). 23

J. A. Gollob, K. Moran, T. Richmond, J. M. Jones, T. E. Baell, W. K. Rathmell, and B. L. Peterson. Phase II trial of sorafenib (BAY 43-9006) in combination with interferon alpha 2b in patients with metastatic renal cell carcinoma. *Ejc Supplements*, 3(2):226–227, Oct. 2005. doi: 10.1016/S1359-6349(05)81088-2. URL [http://dx.doi.org/10.1016/S1359-6349\(05\)81088-2](http://dx.doi.org/10.1016/S1359-6349(05)81088-2). 21

F. Grosjean, M. Huche, M. Larcheveque, J. J. Legendre, and Y. Petit. Etude par la modelisation moleculaire de la regioselectivite de l’Ouverture des acides glycidiques par les amines aliphatiques. *Tetrahedron*, 50(31):9325–9334, 1994. URL <http://www.sciencedirect.com/science/article/B6THR-42GDSWV-6J/2/48240e503ac7ac6f5f492a3befd39450>. 42, 43, 63

C. A. Hall-Jackson, P. A. Eyers, P. Cohen, M. Goedert, F. T. Boyle, N. Hewitt, H. Plant, and P. Hedge. Paradoxical activation of Raf by a novel Raf inhibitor. *Chem Biol*, 6(8):559–568, Aug 1999a. 28, 45

C. A. Hall-Jackson, M. Goedert, P. Hedge, and P. Cohen. Effect of SB 203580 on the activity of c-Raf in vitro and in vivo. *Oncogene*, 18(12):2047–2054, Mar 1999b. doi: 10.1038/sj.onc.1202603. URL <http://dx.doi.org/10.1038/sj.onc.1202603>. 28, 45, 64, 65

G. Heidecker, W. Köhler, D. K. Morrison, and U. R. Rapp. The role of Raf-1 phosphorylation in signal transduction. *Adv Cancer Res*, 58:53–73, 1992. 33

R. Heinrich, B. G. Neel, and T. A. Rapoport. Mathematical models of protein kinase signal transduction. *Mol Cell*, 9(5):957–970, May 2002. doi: 10.1016/S1097-2765(02)00528-2. URL [http://dx.doi.org/10.1016/S1097-2765\(02\)00528-2](http://dx.doi.org/10.1016/S1097-2765(02)00528-2). 29, 49, 52, 55, 66

M. Hekman, H. Hamm, A. V. Villar, B. Bader, J. Kuhlmann, J. Nickel, and U. R. Rapp. Associations of B- and C-Raf with cholesterol, phosphatidylserine, and lipid second messengers: preferential binding of Raf to artificial lipid rafts. *J Biol Chem*, 277(27):24090–24102, Jul 2002. doi: 10.1074/jbc.M200576200. URL <http://dx.doi.org/10.1074/jbc.M200576200>. 36

M. Hekman, S. Wiese, R. Metz, S. Albert, J. Troppmair, J. Nickel, M. Sendtner, and U. R. Rapp. Dynamic changes in C-Raf phosphorylation and 14-3-3 protein binding in response to growth factor stimulation: differential roles of 14-3-3 protein binding sites. *J Biol Chem*, 279(14):14074–14086, Apr 2004. doi: 10.1074/jbc.M309620200. URL <http://dx.doi.org/10.1074/jbc.M309620200>. 25

M. Hekman, A. Fischer, L. P. Wennogle, Y. K. Wang, S. L. Campbell, and U. R. Rapp. Novel C-Raf phosphorylation sites: serine 296 and 301 participate in Raf regulation. *FEBS Lett*, 579(2):464–468, Jan 2005. doi: 10.1016/j.febslet.2004.11.105. URL <http://dx.doi.org/10.1016/j.febslet.2004.11.105>. 24, 64, 65, 66

H. Hisatomi, K. Nagao, K. Wakita, and N. Kohno. ARHI/NOEY2 inactivation may be important in breast tumor pathogenesis. *Oncology*, 62(2):136–140, 2002. doi: 10.1159/000048259. URL <http://dx.doi.org/10.1159/000048259>. 30

R. Hoshino, Y. Chatani, T. Yamori, T. Tsuruo, H. Oka, O. Yoshida, Y. Shimada, S. Ari-i, H. Wada, J. Fujimoto, and M. Kohno. Constitutive activation of the 41-/43-kDa mitogen-activated protein kinase signaling pathway in human tumors. *Oncogene*, 18(3):813–822, Jan 1999. doi: 10.1038/sj.onc.1202367. URL <http://dx.doi.org/10.1038/sj.onc.1202367>. 19, 23

L. R. Howe, S. J. Leever, N. Gómez, S. Nakielny, P. Cohen, and C. J. Marshall. Activation of the MAP kinase pathway by the protein kinase raf. *Cell*, 71(2):335–342, Oct 1992. doi: 10.1016/0092-8674(92)90361-F. URL [http://dx.doi.org/10.1016/0092-8674\(92\)90361-F](http://dx.doi.org/10.1016/0092-8674(92)90361-F). 22

S. R. Hubbard, L. Wei, L. Ellis, and W. A. Hendrickson. Crystal structure of the tyrosine kinase domain of the human insulin receptor. *Nature*, 372(6508):746–754, 1994. doi: 10.1038/372746a0. URL <http://dx.doi.org/10.1038/372746a0>. 37, 39

K. Huebner, A. ar Rushdi, C. A. Griffin, M. Isobe, C. Kozak, B. S. Emanuel, L. Nagarajan, J. L. Cleveland, T. I. Bonner, and M. D. Goldsborough. Actively transcribed genes in the raf oncogene group, located on the X chromosome in mouse and human. *Proc Natl Acad Sci U S A*, 83(11):3934–3938, Jun 1986. URL <http://www.pubmedcentral.nih.gov/articlerender.fcgi?tool=pubmed&pubmedid=3520560>. 20

S. Ikawa, M. Fukui, Y. Ueyama, N. Tamaoki, T. Yamamoto, and K. Toyoshima. B-raf, a new member of the raf family, is activated

by DNA rearrangement. *Mol Cell Biol*, 8(6):2651–2654, Jun 1988. URL <http://www.pubmedcentral.nih.gov/articlerender.fcgi?tool=pubmed&pubmedid=3043188>. 20

H. W. Jansen, B. Rückert, R. Lurz, and K. Bister. Two unrelated cell-derived sequences in the genome of avian leukemia and carcinoma inducing retrovirus MH2. *EMBO J*, 2(11):1969–1975, 1983. URL <http://www.pubmedcentral.nih.gov/articlerender.fcgi?tool=pubmed&pubmedid=6315409>. 20

H. W. Jansen, R. Lurz, K. Bister, T. I. Bonner, G. E. Mark, and U. R. Rapp. Homologous cell-derived oncogenes in avian carcinoma virus MH2 and murine sarcoma virus 3611. *Nature*, 307(5948):281–284, 1984. doi: 10.1038/307281a0. URL <http://dx.doi.org/10.1038/307281a0>. 20

E. Kerkhoff and U. R. Rapp. Induction of cell proliferation in quiescent NIH 3T3 cells by oncogenic c-Raf-1. *Mol Cell Biol*, 17(5):2576–2586, May 1997. URL <http://www.pubmedcentral.nih.gov/articlerender.fcgi?tool=pubmed&pubmedid=9111327>. 30

E. Kerkhoff and U. R. Rapp. High-intensity Raf signals convert mitotic cell cycling into cellular growth. *Cancer Res*, 58(8):1636–1640, Apr 1998. URL <http://cancerres.aacrjournals.org/cgi/content/abstract/58/8/1636>. 29, 30

H. Koide, T. Satoh, M. Nakafuku, and Y. Kaziro. GTP-dependent association of Raf-1 with Ha-Ras: identification of Raf as a target downstream of Ras in mammalian cells. *Proc Natl Acad Sci U S A*, 90(18):8683–8686, Sep 1993. URL <http://www.pubmedcentral.nih.gov/articlerender.fcgi?tool=pubmed&pubmedid=8378348>. 21, 22

B. W. Kramer, R. Götz, and U. R. Rapp. Use of mitogenic cascade blockers for treatment of C-Raf induced lung adenoma in vivo: CI-1040 strongly reduces growth and improves lung structure. *BMC Cancer*, 4:24, Jun 2004. doi: 10.1186/1471-2407-4-24. URL <http://dx.doi.org/10.1186/1471-2407-4-24>. 66

M. Kubicek, M. Pacher, D. Abraham, K. Podar, M. Eulitz, and M. Baccarini. Dephosphorylation of Ser-259 regulates Raf-1 membrane association. *J Biol Chem*, 277(10):7913–7919, Mar 2002. doi: 10.1074/jbc.M108733200. URL <http://dx.doi.org/10.1074/jbc.M108733200>. 58

J. M. Kyriakis, H. App, X. F. Zhang, P. Banerjee, D. L. Brautigan, U. R. Rapp, and J. Avruch. Raf-1 activates MAP kinase-kinase. *Nature*, 358(6385):

417–421, Jul 1992. doi: 10.1038/358417a0. URL <http://dx.doi.org/10.1038/358417a0>. 22

K. Lackey, M. Cory, R. Davis, S. V. Frye, P. A. Harris, R. N. Hunter, D. K. Jung, O. B. McDonald, R. W. McNutt, M. R. Peel, R. D. Rutkowske, J. M. Veal, and E. R. Wood. The discovery of potent cRaf1 kinase inhibitors. *Bioorg Med Chem Lett*, 10(3):223–226, Feb 2000. doi: 10.1016/S0960-894X(99)00668-X. URL [http://dx.doi.org/10.1016/S0960-894X\(99\)00668-X](http://dx.doi.org/10.1016/S0960-894X(99)00668-X). 28, 45

J. Lew. MAP kinases and CDKs: kinetic basis for catalytic activation. *Biochemistry*, 42(4):849–856, Feb 2003. doi: 10.1021/bi0269761. URL <http://dx.doi.org/10.1021/bi0269761>. 51, 52, 55

T. B. Lowinger, B. Riedl, J. Dumas, and R. A. Smith. Design and discovery of small molecules targeting raf-1 kinase. *Curr Pharm Des*, 8(25):2269–2278, 2002. doi: 10.2174/1381612023393125. URL <http://dx.doi.org/10.2174/1381612023393125>. 20, 21

Z. Lu, R. Z. Luo, H. Peng, D. G. Rosen, E. N. Atkinson, C. Warneke, M. Huang, A. Nishimoto, J. Liu, W. S.-L. Liao, Y. Yu, and R. C. Bast. Transcriptional and posttranscriptional down-regulation of the imprinted tumor suppressor gene ARHI (DRAS3) in ovarian cancer. *Clin Cancer Res*, 12(8):2404–2413, Apr 2006. doi: 10.1158/1078-0432.CCR-05-1036. URL <http://dx.doi.org/10.1158/1078-0432.CCR-05-1036>. 30, 31

R. Z. Luo, X. Fang, R. Marquez, S.-Y. Liu, G. B. Mills, W. S.-L. Liao, Y. Yu, and R. C. Bast. ARHI is a Ras-related small G-protein with a novel N-terminal extension that inhibits growth of ovarian and breast cancers. *Oncogene*, 22(19):2897–2909, May 2003. doi: 10.1038/sj.onc.1206380. URL <http://dx.doi.org/10.1038/sj.onc.1206380>. 30, 31

Z. Luo, G. Tzivion, P. J. Belshaw, D. Vavvas, M. Marshall, and J. Avruch. Oligomerization activates c-Raf-1 through a Ras-dependent mechanism. *Nature*, 383(6596):181–185, Sep 1996. doi: 10.1038/383181a0. URL <http://dx.doi.org/10.1038/383181a0>. 45

M. Malumbres and M. Barbacid. RAS oncogenes: the first 30 years. *Nat Rev Cancer*, 3(6):459–465, Jun 2003. doi: 10.1038/nrc1097. URL <http://dx.doi.org/10.1038/nrc1097>. 21, 23

C. J. Marshall. Specificity of receptor tyrosine kinase signaling: transient versus sustained extracellular signal-regulated kinase activation. *Cell*, 80

(2):179–185, Jan 1995. URL <http://www.cell.com/content/article/abstract?uid=PII0092867495904018>. 29, 30

C. S. Mason, C. J. Springer, R. G. Cooper, G. Superti-Furga, C. J. Marshall, and R. Marais. Serine and tyrosine phosphorylations cooperate in Raf-1, but not B-Raf activation. *EMBO J*, 18(8):2137–2148, Apr 1999. doi: 10.1093/emboj/18.8.2137. URL <http://dx.doi.org/10.1093/emboj/18.8.2137>. 58

M. M. McKay and D. K. Morrison. Integrating signals from RTKs to ERK/MAPK. *Oncogene*, 26(22):3113–3121, May 2007. doi: 10.1038/sj.onc.1210394. URL <http://dx.doi.org/10.1038/sj.onc.1210394>. 69

M. Mikula, M. Schreiber, Z. Husak, L. Kucerova, J. R uth, R. Wieser, K. Zatloukal, H. Beug, E. F. Wagner, and M. Baccarini. Embryonic lethality and fetal liver apoptosis in mice lacking the c-raf-1 gene. *EMBO J*, 20(8):1952–1962, Apr 2001. doi: 10.1093/emboj/20.8.1952. URL <http://dx.doi.org/10.1093/emboj/20.8.1952>. 23

V. Neuhoff, N. Arold, D. Taube, and W. Ehrhardt. Improved staining of proteins in polyacrylamide gels including isoelectric focusing gels with clear background at nanogram sensitivity using Coomassie Brilliant Blue G-250 and R-250. *Electrophoresis*, 9(6):255–262, Jun 1988. doi: 10.1002/elps.1150090603. URL <http://dx.doi.org/10.1002/elps.1150090603>. 37

M. Offterdinger, V. Georget, A. Girod, and P. I. H. Bastiaens. Imaging phosphorylation dynamics of the epidermal growth factor receptor. *J Biol Chem*, 279(35):36972–36981, Aug 2004. doi: 10.1074/jbc.M405830200. URL <http://dx.doi.org/10.1074/jbc.M405830200>. 67

G. Pag es, S. Gu erin, D. Grall, F. Bonino, A. Smith, F. Anjuere, P. Auberger, and J. Pouyssegur. Defective thymocyte maturation in p44 MAP kinase (Erk 1) knockout mice. *Science*, 286(5443):1374–1377, Nov 1999. doi: 10.1126/science.286.5443.1374. URL <http://dx.doi.org/10.1126/science.286.5443.1374>. 22

C. Pargellis, L. Tong, L. Churchill, P. F. Cirillo, T. Gilmore, A. G. Graham, P. M. Grob, E. R. Hickey, N. Moss, S. Pav, and J. Regan. Inhibition of p38 MAP kinase by utilizing a novel allosteric binding site. *Nat Struct Biol*, 9(4):268–272, Apr 2002. doi: 10.1038/nsb770. URL <http://dx.doi.org/10.1038/nsb770>. 37, 39, 45

D. M. Payne, A. J. Rossomando, P. Martino, A. K. Erickson, J. H. Her, J. Shabanowitz, D. F. Hunt, M. J. Weber, and T. W. Sturgill.

Identification of the regulatory phosphorylation sites in pp42/mitogen-activated protein kinase (MAP kinase). *EMBO J*, 10(4):885–892, Apr 1991. URL <http://www.pubmedcentral.nih.gov/articlerender.fcgi?tool=pubmed&pubmedid=1849075>. 22

A. Peyker, O. Rocks, and P. I. H. Bastiaens. Imaging activation of two Ras isoforms simultaneously in a single cell. *Chembiochem*, 6(1):78–85, Jan 2005. doi: 10.1002/cbic.200400280. URL <http://dx.doi.org/10.1002/cbic.200400280>. 67

K. E. Prehoda, J. A. Scott, R. D. Mullins, and W. A. Lim. Integration of multiple signals through cooperative regulation of the N-WASP-Arp2/3 complex. *Science*, 290(5492):801–806, Oct 2000. doi: 10.1126/science.290.5492.801. URL <http://dx.doi.org/10.1126/science.290.5492.801>. 69

I. A. Prior, A. Harding, J. Yan, J. Sluimer, R. G. Parton, and J. F. Hancock. GTP-dependent segregation of H-ras from lipid rafts is required for biological activity. *Nat Cell Biol*, 3(4):368–375, Apr 2001. doi: 10.1038/35070050. URL <http://dx.doi.org/10.1038/35070050>. 70

C. A. Pritchard, L. Bolin, R. Slattery, R. Murray, and M. McMahon. Post-natal lethality and neurological and gastrointestinal defects in mice with targeted disruption of the A-Raf protein kinase gene. *Curr Biol*, 6(5):614–617, May 1996. doi: 10.1016/S0960-9822(02)00548-1. URL [http://dx.doi.org/10.1016/S0960-9822\(02\)00548-1](http://dx.doi.org/10.1016/S0960-9822(02)00548-1). 23

M. S. Qui and S. H. Green. PC12 cell neuronal differentiation is associated with prolonged p21ras activity and consequent prolonged ERK activity. *Neuron*, 9(4):705–717, Oct 1992. URL <http://www.neuron.org/content/article/abstract?uid=PII089662739290033A>. 29, 52, 55

U. R. Rapp, M. D. Goldsborough, G. E. Mark, T. I. Bonner, J. Groffen, F. H. Reynolds, and J. R. Stephenson. Structure and biological activity of v-raf, a unique oncogene transduced by a retrovirus. *Proc Natl Acad Sci U S A*, 80(14):4218–4222, Jul 1983. URL <http://www.pubmedcentral.nih.gov/articlerender.fcgi?tool=pubmed&pubmedid=6308607>. 19, 20

U. E. E. Rennefahrt, B. Illert, E. Kerkhoff, J. Troppmair, and U. R. Rapp. Constitutive JNK activation in NIH 3T3 fibroblasts induces a partially transformed phenotype. *J Biol Chem*, 277(33):29510–29518, Aug 2002. doi: 10.1074/jbc.M203010200. URL <http://dx.doi.org/10.1074/jbc.M203010200>. 33

H. Richly, P. Kupsch, K. Passage, M. Grubert, R. A. Hilger, S. Kredtke, D. Voliotis, M. E. Scheulen, S. Seeber, and D. Strumberg. A phase I clinical and pharmacokinetic study of the Raf kinase inhibitor (RKI) BAY 43-9006 administered in combination with doxorubicin in patients with solid tumors. *Int J Clin Pharmacol Ther*, 41(12):620–621, Dec 2003. URL <http://www.dustri.com/ze/cp/samplecopy/cp12620.pdf>. 21

D. J. Robbins, E. Zhen, H. Owaki, C. A. Vanderbilt, D. Ebert, T. D. Geppert, and M. H. Cobb. Regulation and properties of extracellular signal-regulated protein kinases 1 and 2 in vitro. *J Biol Chem*, 268(7):5097–5106, Mar 1993. URL <http://www.jbc.org/cgi/content/abstract/268/7/5097>. 22

A. Robubi, T. Mueller, J. Fueller, M. Hekman, U. R. Rapp, and T. Dandekar. B-Raf and C-Raf signaling investigated in a simplified model of the mitogenic kinase cascade. *Biol Chem*, 386(11):1165–1171, Nov 2005. doi: 10.1515/BC.2005.133. URL <http://dx.doi.org/10.1515/BC.2005.133>. VI, VIII, 36, 55

P. Rodriguez-Viciana, O. Tetsu, W. E. Tidymann, A. L. Estep, B. A. Conger, M. S. Cruz, F. McCormick, and K. A. Rauen. Germline mutations in genes within the MAPK pathway cause cardio-facio-cutaneous syndrome. *Science*, 311(5765):1287–1290, Mar 2006. doi: 10.1126/science.1124642. URL <http://dx.doi.org/10.1126/science.1124642>. 22

D. G. Rosen, L. Wang, A. N. Jain, K. H. Lu, R. Z. Luo, Y. Yu, J. Liu, and R. C. Bast. Expression of the tumor suppressor gene ARHI in epithelial ovarian cancer is associated with increased expression of p21WAF1/CIP1 and prolonged progression-free survival. *Clin Cancer Res*, 10(19):6559–6566, Oct 2004. doi: 10.1158/1078-0432.CCR-04-0698. URL <http://dx.doi.org/10.1158/1078-0432.CCR-04-0698>. 30

L. K. Rushworth, A. D. Hindley, E. O’Neill, and W. Kolch. Regulation and role of Raf-1/B-Raf heterodimerization. *Mol Cell Biol*, 26(6):2262–2272, Mar 2006. doi: 10.1128/MCB.26.6.2262-2272.2006. URL <http://dx.doi.org/10.1128/MCB.26.6.2262-2272.2006>. 45, 46, 64

M. K. Saba-El-Leil, F. D. J. Vella, B. Vernay, L. Voisin, L. Chen, N. Labrecque, S.-L. Ang, and S. Meloche. An essential function of the mitogen-activated protein kinase Erk2 in mouse trophoblast development. *EMBO Rep*, 4(10):964–968, Oct 2003. doi: 10.1038/sj.embor.embor939. URL <http://dx.doi.org/10.1038/sj.embor.embor939>. 22

A. Sali and T. L. Blundell. Comparative protein modelling by satisfaction of spatial restraints. *J Mol Biol*, 234(3):779–815, Dec 1993. doi: 10.1006/jmbi.1993.1626. URL <http://dx.doi.org/10.1006/jmbi.1993.1626>. 37, 39

S. Sasagawa, Y. ichi Ozaki, K. Fujita, and S. Kuroda. Prediction and validation of the distinct dynamics of transient and sustained ERK activation. *Nat Cell Biol*, 7(4):365–373, Apr 2005. doi: 10.1038/ncb1233. URL <http://dx.doi.org/10.1038/ncb1233>. 67

I. Schomburg, A. Chang, C. Ebeling, M. Gremse, C. Heldt, G. Huhn, and D. Schomburg. BRENDA, the enzyme database: updates and major new developments. *Nucleic Acids Res*, 32(Database issue):D431–D433, Jan 2004. doi: 10.1093/nar/gkh081. URL <http://dx.doi.org/10.1093/nar/gkh081>. 53

A. Sewing, B. Wiseman, A. C. Lloyd, and H. Land. High-intensity Raf signal causes cell cycle arrest mediated by p21Cip1. *Mol Cell Biol*, 17(9):5588–5597, Sep 1997. URL <http://www.pubmedcentral.nih.gov/articlerender.fcgi?tool=pubmed&pubmedid=9271434>. 30

G. Sithanandam, T. Druck, L. A. Cannizzaro, G. Leuzzi, K. Huebner, and U. R. Rapp. B-raf and a B-raf pseudogene are located on 7q in man. *Oncogene*, 7(4):795–799, Apr 1992. 20

S. M. Storm, J. L. Cleveland, and U. R. Rapp. Expression of raf family proto-oncogenes in normal mouse tissues. *Oncogene*, 5(3):345–351, Mar 1990. 66

D. Strumberg, J. W. Clark, A. Awada, M. J. Moore, H. Richly, A. Hendlisz, H. W. Hirte, J. P. Eder, H.-J. Lenz, and B. Schwartz. Safety, pharmacokinetics, and preliminary antitumor activity of sorafenib: a review of four phase I trials in patients with advanced refractory solid tumors. *Oncologist*, 12(4):426–437, Apr 2007. doi: 10.1634/theoncologist.12-4-426. URL <http://dx.doi.org/10.1634/theoncologist.12-4-426>. 20, 21

R. M. Tombes, K. L. Auer, R. Mikkelsen, K. Valerie, M. P. Wymann, C. J. Marshall, M. McMahon, and P. Dent. The mitogen-activated protein (MAP) kinase cascade can either stimulate or inhibit DNA synthesis in primary cultures of rat hepatocytes depending upon whether its activation is acute/phasic or chronic. *Biochem J*, 330 (Pt 3):1451–1460, Mar 1998. URL <http://www.pubmedcentral.nih.gov/articlerender.fcgi?tool=pubmed&pubmedid=9494119>. 29, 30

N. Trakul, R. E. Menard, G. R. Schade, Z. Qian, and M. R. Rosner. Raf kinase inhibitory protein regulates Raf-1 but not B-Raf kinase activation. *J Biol Chem*, 280(26):24931–24940, Jul 2005. doi: 10.1074/jbc.M413929200. URL <http://dx.doi.org/10.1074/jbc.M413929200>. 68

P. T. C. Wan, M. J. Garnett, S. M. Roe, S. Lee, D. Niculescu-Duvaz, V. M. Good, C. M. Jones, C. J. Marshall, C. J. Springer, D. Barford, R. Marais, and C. G. Project. Mechanism of activation of the RAF-ERK signaling pathway by oncogenic mutations of B-RAF. *Cell*, 116(6):855–867, Mar 2004. doi: 10.1016/S0092-8674(04)00215-6. URL [http://dx.doi.org/10.1016/S0092-8674\(04\)00215-6](http://dx.doi.org/10.1016/S0092-8674(04)00215-6). 25, 27, 39, 40, 45

L. Wang, A. Hoque, R. Z. Luo, J. Yuan, Z. Lu, A. Nishimoto, J. Liu, A. A. Sahin, S. M. Lippman, R. C. Bast, and Y. Yu. Loss of the expression of the tumor suppressor gene ARHI is associated with progression of breast cancer. *Clin Cancer Res*, 9(10 Pt 1):3660–3666, Sep 2003. URL <http://clincancerres.aacrjournals.org/cgi/content/full/9/10/3660>. 30

C. Wellbrock, M. Karasarides, and R. Marais. The RAF proteins take centre stage. *Nat Rev Mol Cell Biol*, 5(11):875–885, Nov 2004. doi: 10.1038/nrm1498. URL <http://dx.doi.org/10.1038/nrm1498>. 20

S. M. Wilhelm, C. Carter, L. Tang, D. Wilkie, A. McNabola, H. Rong, C. Chen, X. Zhang, P. Vincent, M. McHugh, Y. Cao, J. Shujath, S. Gawlak, D. Eveleigh, B. Rowley, L. Liu, L. Adnane, M. Lynch, D. Auclair, I. Taylor, R. Gedrich, A. Voznesensky, B. Riedl, L. E. Post, G. Bollag, and P. A. Trail. BAY 43-9006 exhibits broad spectrum oral antitumor activity and targets the RAF/MEK/ERK pathway and receptor tyrosine kinases involved in tumor progression and angiogenesis. *Cancer Res*, 64(19):7099–7109, Oct 2004. doi: 10.1158/0008-5472.CAN-04-1443. URL <http://dx.doi.org/10.1158/0008-5472.CAN-04-1443>. 21, 64, 65

E. Wilker and M. B. Yaffe. 14-3-3 Proteins—a focus on cancer and human disease. *J Mol Cell Cardiol*, 37(3):633–642, Sep 2004. doi: 10.1016/j.yjmcc.2004.04.015. URL <http://dx.doi.org/10.1016/j.yjmcc.2004.04.015>. 70

M. Wilm, A. Shevchenko, T. Houthaeve, S. Breit, L. Schweigerer, T. Fotsis, and M. Mann. Femtomole sequencing of proteins from polyacrylamide gels by nano-electrospray mass spectrometry. *Nature*, 379(6564):466–469, Feb 1996. doi: 10.1038/379466a0. URL <http://dx.doi.org/10.1038/379466a0>. 37

V. Wixler, U. Smola, M. Schuler, and U. Rapp. Differential regulation of Raf isozymes by growth versus differentiation inducing factors in PC12 pheochromocytoma cells. *FEBS Lett*, 385(3):131–137, May 1996. doi: 10.1016/0014-5793(96)00363-8. URL [http://dx.doi.org/10.1016/0014-5793\(96\)00363-8](http://dx.doi.org/10.1016/0014-5793(96)00363-8). 29, 30

L. Wojnowski, A. M. Zimmer, T. W. Beck, H. Hahn, R. Bernal, U. R. Rapp, and A. Zimmer. Endothelial apoptosis in Braf-deficient mice. *Nat Genet*, 16(3):293–297, Jul 1997. doi: 10.1038/ng0797-293. URL <http://dx.doi.org/10.1038/ng0797-293>. 23

D. Woods, D. Parry, H. Cherwinski, E. Bosch, E. Lees, and M. McMahon. Raf-induced proliferation or cell cycle arrest is determined by the level of Raf activity with arrest mediated by p21Cip1. *Mol Cell Biol*, 17(9):5598–5611, Sep 1997. URL <http://www.pubmedcentral.nih.gov/articlerender.fcgi?tool=pubmed&pubmedid=9271435>. 30

S. Yamada, T. Taketomi, and A. Yoshimura. Model analysis of difference between EGF pathway and FGF pathway. *Biochem Biophys Res Commun*, 314(4):1113–1120, Feb 2004. doi: 10.1016/j.bbrc.2004.01.009. URL <http://dx.doi.org/10.1016/j.bbrc.2004.01.009>. 67

Y. Yu, F. Xu, H. Peng, X. Fang, S. Zhao, Y. Li, B. Cuevas, W. L. Kuo, J. W. Gray, M. Siciliano, G. B. Mills, and R. C. Bast. NOEY2 (ARHI), an imprinted putative tumor suppressor gene in ovarian and breast carcinomas. *Proc Natl Acad Sci U S A*, 96(1):214–219, Jan 1999. URL <http://www.pubmedcentral.nih.gov/articlerender.fcgi?tool=pubmed&pubmedid=9874798>. 30, 31, 69

Y. Yu, R. Luo, Z. Lu, W. W. Feng, D. Badgwell, J.-P. Issa, D. G. Rosen, J. Liu, and R. C. Bast. Biochemistry and Biology of ARHI (DIRAS3), an Imprinted Tumor Suppressor Gene Whose Expression Is Lost in Ovarian and Breast Cancers. *Methods Enzymol*, 407:455–468, 2005. doi: 10.1016/S0076-6879(05)07037-0. URL [http://dx.doi.org/10.1016/S0076-6879\(05\)07037-0](http://dx.doi.org/10.1016/S0076-6879(05)07037-0). 30, 69

A. Zebisch, P. B. Staber, A. Delavar, C. Bodner, K. Hiden, K. Fischereder, M. Janakiraman, W. Linkesch, H. W. Auner, W. Emberger, C. Windpassinger, M. G. Schimek, G. Hoefler, J. Troppmair, and H. Sill. Two transforming C-RAF germ-line mutations identified in patients with therapy-related acute myeloid leukemia. *Cancer Res*, 66(7):3401–3408, Apr 2006. doi: 10.1158/0008-5472.CAN-05-0115. URL <http://dx.doi.org/10.1158/0008-5472.CAN-05-0115>. 22

X. F. Zhang, J. Settleman, J. M. Kyriakis, E. Takeuchi-Suzuki, S. J. Elledge, M. S. Marshall, J. T. Bruder, U. R. Rapp, and J. Avruch. Normal and oncogenic p21ras proteins bind to the amino-terminal regulatory domain of c-Raf-1. *Nature*, 364(6435):308–313, Jul 1993. doi: 10.1038/364308a0. URL <http://dx.doi.org/10.1038/364308a0>. 20, 21, 22

J. Zhong, J. Troppmair, and U. R. Rapp. Independent control of cell survival by Raf-1 and Bcl-2 at the mitochondria. *Oncogene*, 20(35):4807–4816, Aug 2001. doi: 10.1038/sj.onc.1204614. URL <http://dx.doi.org/10.1038/sj.onc.1204614>. 33

X. Zhu, J. L. Kim, J. R. Newcomb, P. E. Rose, D. R. Stover, L. M. Toledo, H. Zhao, and K. A. Morgenstern. Structural analysis of the lymphocyte-specific kinase Lck in complex with non-selective and Src family selective kinase inhibitors. *Structure*, 7(6):651–661, Jun 1999. doi: 10.1016/S0969-2126(99)80086-0. URL [http://dx.doi.org/10.1016/S0969-2126\(99\)80086-0](http://dx.doi.org/10.1016/S0969-2126(99)80086-0). 37, 39

Acknowledgments

I want to thank my thesis board Prof. Dr. Thomas Dandkar (supervisor), Prof. Dr. Ulf R. Rapp (advisor), and Prof. Dr. Shamil Sunyaev (external advisor).

I also want to thank my co-authors Prof. Dr. Claus Herdeis, Mirko Hekman, Jochen Füller, Tobias Müller, Marcus Dittrich, Ruth Kroschewski, Mirko Klingauf, Matthias Beck, Stephan Heinzer, Yagmur Turgayand, and Werner Schmitz

... and many other people for their support: Ulrike Rennefahrt, Andreas Fischer, Birgit Pils, Elena Nekhoroshkova, Stefan Albert, Barbara Bauer, Ludmilla Wixler, Tina Schüll, Maureen Menning, Renate Metz, and Frank Förster.

I gratefully acknowledge funding by the Bavarian state (BIGSS elite network; IZKF grant B-36) and the BMBF (Systems Biology grant 03 130 74D).

Curriculum vitae

Name	Robubi
Given Name	Armin
Previous name	Robobi
Postal address	Lange Bögen 2, D-97074 Würzburg, Germany
Phone	+49-931-2969754
Email	me@armin.eu.org

Personal data

Date of birth	Sep. 22 nd , 1977
Place of birth	Tehran, Iran
Marital status	unmarried
Children	none
Nationality	Austrian

Education

Lower education

1984–1988	Primary school, Vienna, Austria
1988–1996	Grammar school, Vienna, Austria
1996	School leaving examination (Matura)

Higher Education

1996–2000	Chemical Engineering, Technical University of Vienna (TU-Wien), Vienna, Austria
2000–2002	Masters Program of Bioinformatics, Chalmers, Göteborg, Sweden
August 2002	Masters of Science in Bioinformatics, Supervisor: Dr. Per-Georg Nyholm, Structural chemistry group, Department of Medical Chemistry, University of Göteborg (GU), Göteborg, Sweden
Sep. 2002–Sep. 2004	Research project, Supervisor: Prof. Dr. Ulf R. Rapp, Protein group, Institute for Medical Radiation and Cell Research, University of Würzburg, Würzburg, Germany
October 2004–present	Thesis project – BioMedTec Franken International Graduate School (BIGSS)—Elite Network of Bavaria, Supervisor: Prof. Dr. Thomas Dandekar, Department of Bioinformatics, University of Würzburg, Würzburg, Germany

List of publications

- Beck M, Robubi A, Klingauf M, Hekman M, Heinzer S, Turgay Y, Rapp U. R, Kroschewski R. ‘The Ras-like tumor suppressor DiRas3 (Noey2, ARHI) downregulates specifically the RAF-MEK-ERK signaling pathway by inhibiting MEK’ *Molecular Cell*–submitted.
- Robubi A, Schmitz W, Herdeis C, Rapp U. R, Dandekar T. ‘A proof-of-concept study with a novel diphenyl urea lead compound to irreversibly inhibit the Cys109 protein kinase and oncoprotein RAF: design, synthesis, activity *in vitro* and *in vivo*.’ *ChemMedChem*–submitted.
- Robubi A, Mueller T, Fueller J, Hekman M, Rapp U. R, Dandekar T. ‘B-Raf and C-Raf signaling investigated in a simplified model of the mitogenic kinase cascade.’ *Biological Chemistry* 386 (2005) 1165–1171. DOI: 10.1515/BC.2005.133
- Rosen J, Robubi A, Nyholm PG. ‘The conformations of the O-specific polysaccharides of *Shigella dysenteriae* type 4 and *Escherichia coli* O159 studied with molecular mechanics (MM3) filtered systematic search.’ *Carbohydrate Research* 339 (2004) 961–966. DOI: 10.1016/j.carres.2003.11.018
- Rosen J, Robubi A, Nyholm PG. ‘Conformation of the branched O-specific polysaccharide of *Shigella dysenteriae* type 2.’ *Carbohydrate Research* 337 (2002) 1633–1640. DOI: 10.1016/S0008-6215(02)00089-7
- Conformational studies on the O-antigens of some gram negative bacteria (Master thesis).
<http://www.math.chalmers.se/Stat/Bioinfo/Master/Theses/2002/7.pdf>

Poster Abstracts

- Robubi, A., Schmitz, W., Herdeis, C., Rapp, U.R., and Dandekar, T. 'A novel diphenyl urea lead compound to irreversibly inhibit the Cys109 protein kinase and oncoprotein RAF: design, synthesis, activity *in vitro* and *in vivo*.' Cancer Genomics and Epigenomics (Keystone), Feb 19–24 2008. Taos, New Mexico, USA.
- Walter, D., Kreutz, C., Neubert, K., McNelly, S., von Weizsäcker, F., Timmer, J., Robubi, A. 'Complex regulation of caspase-3 processing and activity in Fas/CD95L-treated primary mouse hepatocytes.' Conference on Systems Biology of Mammalian Cells (SBMC), Jul 12–14 2006. Heidelberg, Germany.
- Robubi, A., 'Structural basis of Raf Kinase Mutations and Raf Kinase inhibitors.' HUGO's 10th Annual Genome Meeting HGM2005, Apr 18–21 2005. Kyoto, Japan.
- Robubi, A., Dandekar, T., Herdeis, C., Rapp, U.R. 'Structural basis of Raf Kinase Mutations and Raf Kinase Inhibitors.' Ras-dependent pathways in human cancer, Nov 28–Dec 1 2004. Kloster Banz, Germany.
- Robubi, A., Hekman, M., Fischer, A., Albert, S., Rapp, U.R., Wiese, S. 'Regulation of Raf protein kinases by 14-3-3 proteins and KSR.' ELSO 2004, Sep 4–8 2004, Nice, France.
- Robubi, A., Rapp, U.R., Dandekar, T. 'Mitogen activated protein kinase pathways: Improving bioinformatical strategies for inhibitor screening.' Deutsche Pharmazeutischen Gesellschaft (DPhG), Oct 8–11 2003, Würzburg, Germany
- Rosen, J., Robubi A., Nyholm, PG. 'Conformation of the branched O-specific polysaccharide of *Shigella dysenteriae* type 2.' Eurocarb Sep 2–11 2001, Lisbon, Portugal

Oral presentations

- ‘Modeling of the Raf signaling pathway.’, Bioinformatics Symposium. Jul 27, Würzburg, Germany.
- ‘Structural basis of Raf Kinase Mutations and Raf Kinase Inhibitors.’, Rabensteiner Kolleg, May 26–28, Pottenstein, Germany.


Würzburg, December 12, 2007


(Armin Robubi)


Appendix A

Supplementary material

This section also includes supplements, which are too large to be printed in the final thesis. They can only be accessed in the electronic PDF version of the doctoral thesis using a PDF viewer that supports file attachment such as Adobe Reader 4.0 or higher.

 model.pdb.gz: this file contains the homology model of the kinase domain of B-RAF in complex with compound **1** (PDB format compressed with GZIP).

 scripts.zip: contains a set of Matlab files. These scripts—and the parameters therein—were used for our bioinformatics models of the RAF signaling pathway.

 thr106.aln: list of all protein kinases in the human genome with a threonine—or any other amino acid with small side chain—at position 106 (p38 α MAP kinase numbering).

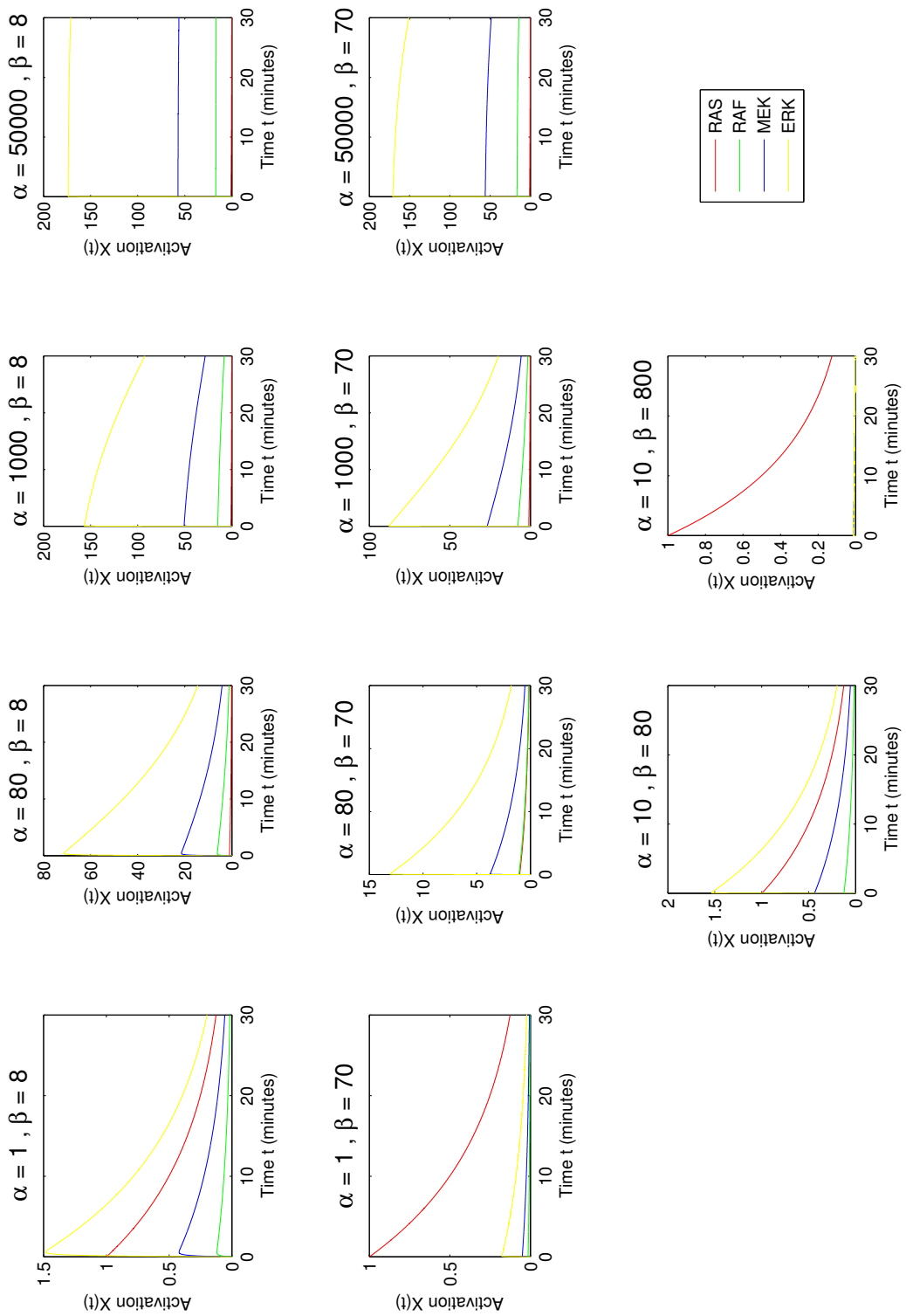


Figure A.1: Scanning different parameter values.

Erklärung

Ich erkläre, dass ich die vorgelegte Dissertation selbständig angefertigt und keine anderen als die angegebenen Quellen und Hilfsmittel benutzt habe.

Weiterhin erkläre ich, dass die vorgelegte Arbeit noch in keinem anderen Prüfungsverfahren in gleicher oder ähnlicher Form vorgelegen hat.

Außer den in dem Zulassungsgesuch urkundlich vorgelegten Graden habe ich keine weiteren Grade erworben oder zu erwerben versucht.

Würzburg, 12. Dezember 2007

(Armin Robubi)